Fundamental Parameters of Stellar (Photospheric) Physics

Jason Aufdenberg (ERAU)

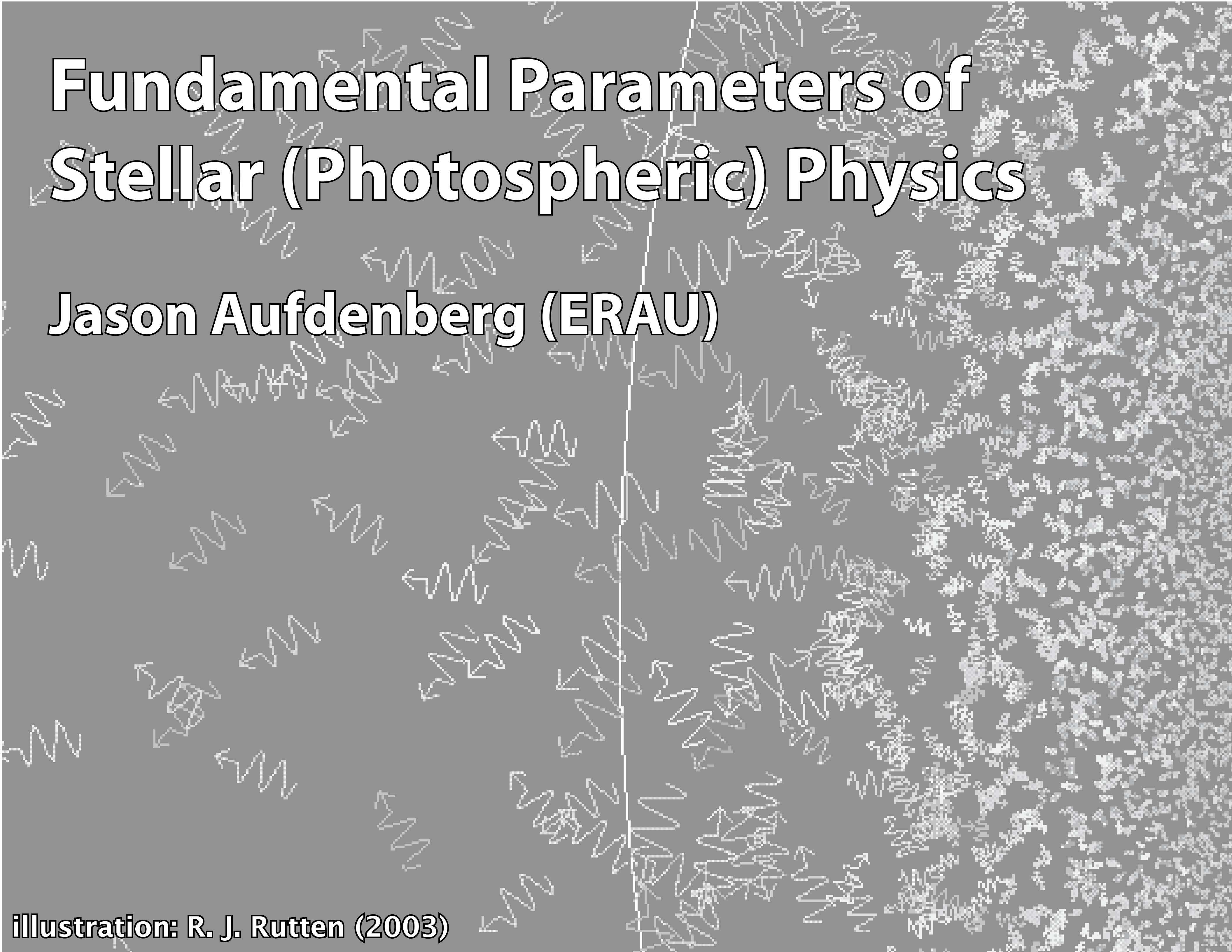

illustration: R. J. Rutten (2003)

What's to Come....

90 Years of stellar angular diameters

Diameters + Distances → Radii

Quick intro to temperature structure of the Sun

Quick introduction to limb darkening

How an interferometer sees a star

Limb darkening observed on 23 stars

Giants, geometry, and limb darkening

Convection, 3D models, and limb darkening

Warm supergiants and limb darkening

Rapid Rotators: observations and models

Michelson and Pease (1921): Angular Size of Betelgeuse
Astrophysical Journal 53, 249-259

MEASUREMENT OF THE DIAMETER OF α ORIONIS WITH THE INTERFEROMETER[1]

By A. A. MICHELSON and F. G. PEASE

ABSTRACT

Twenty-foot interferometer for measuring minute angles.—Since pencils of rays at least 10 feet apart must be used to measure the diameters of even the largest stars, and because the interferometer results obtained with the 100-inch reflector were so encouraging, the construction of a 20-foot interferometer was undertaken. A very rigid beam made of structural steel was mounted on the end of the Cassegrain cage, and four 6-inch mirrors were mounted on it so as to reduce the separation of the pencils to 45 inches and enable them to be brought to accurate coincidence by the telescope. The methods of making the fine adjustments necessary are described, including the use of two thin wedges of glass to vary continuously the equivalent air-path of one pencil. Sharp fringes were obtained with this instrument in August, 1920.

Diameter of α Orionis.—Although the interferometer was not yet provided with means for continuously altering the distance between the pencils used, some observations were made on this star, which was known to be very large. On December 13, 1920, with very good seeing, no fringes could be found when the separation of the pencils was 121 inches, although tests on other stars showed the instrument to be in perfect adjustment. This separation for minimum visibility gives the angular diameter as 0".047 within 10 per cent, assuming the disk of the star uniformly luminous. Hence, taking the parallax as 0".018, the linear diameter comes out 240×10^6 miles.

Interferometer method of determining the distribution of luminosity on a stellar disk.—The variation of intensity of the interference fringes with the separation of the two pencils depends not only on the angular diameter of the disk but also on the distribution of luminosity. The theory is developed for the case in which $I=I_0\,(R^2-r^2)^n$, and formulae are given for determining n from observations.

Table of values of $\int_0^1 (1-x^2)^{n+\frac{1}{2}} \cos kx\, dx$, for n equal to 0, $\frac{1}{2}$, 1, and 2, and for k up to 600°, is given.

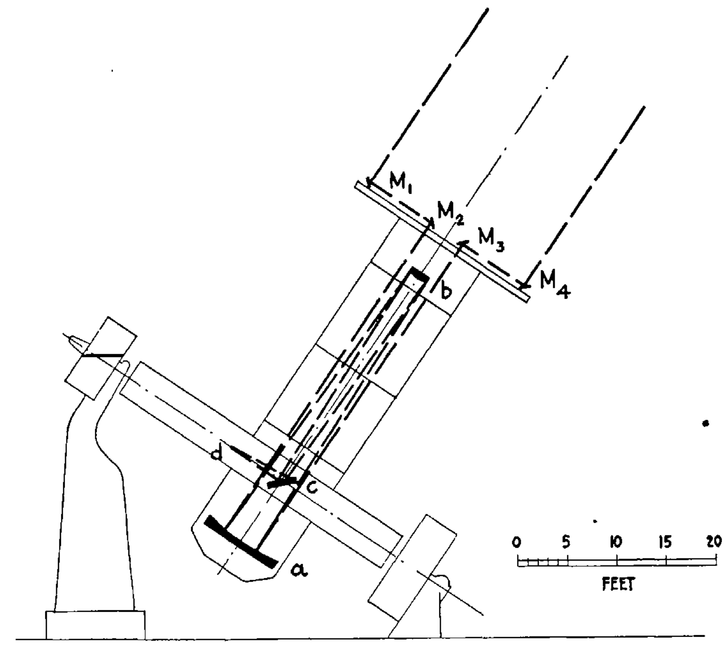

FIG. 1.—Diagram of optical path of interferometer pencils. M_1, M_2, M_3, M_4, mirrors; a, 100-inch paraboloid; b, convex mirror; c, coudé flat; d, focus.

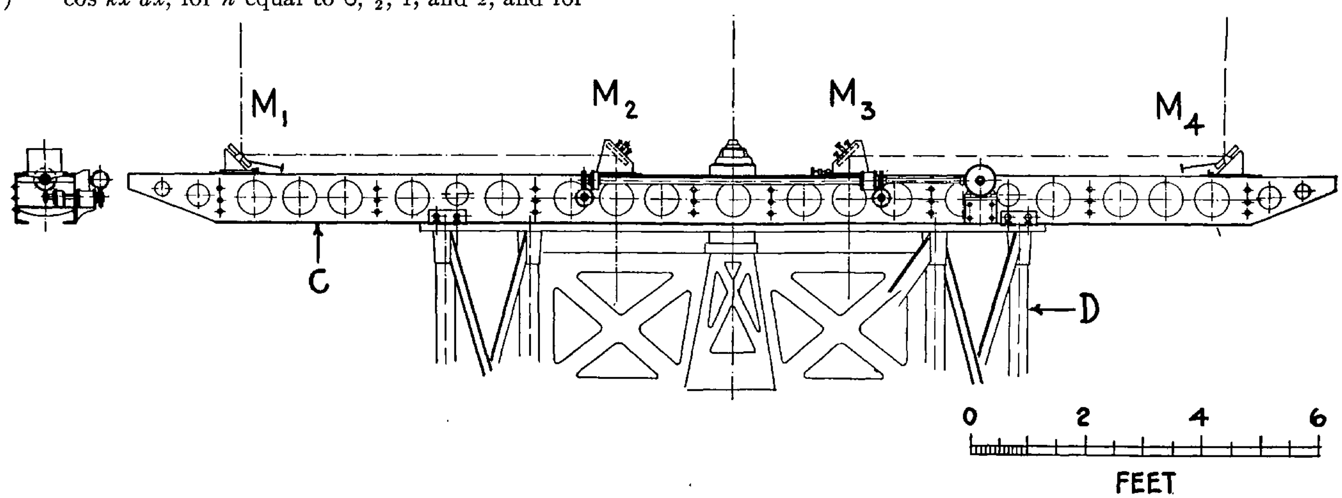

Interferometric Fringes from Creekside Observatory, Daytona Beach, Florida, USA

α Lyrae 29 September 2011

Wavelength: R-band (~600 nm)

Apertures: 12.1 cm, Baseline: 37.5 cm

Scale = 0.08 arcseconds/pixel

0.05 sec exposures, 5 frames per second movie

Radius from Angular Size and Distance

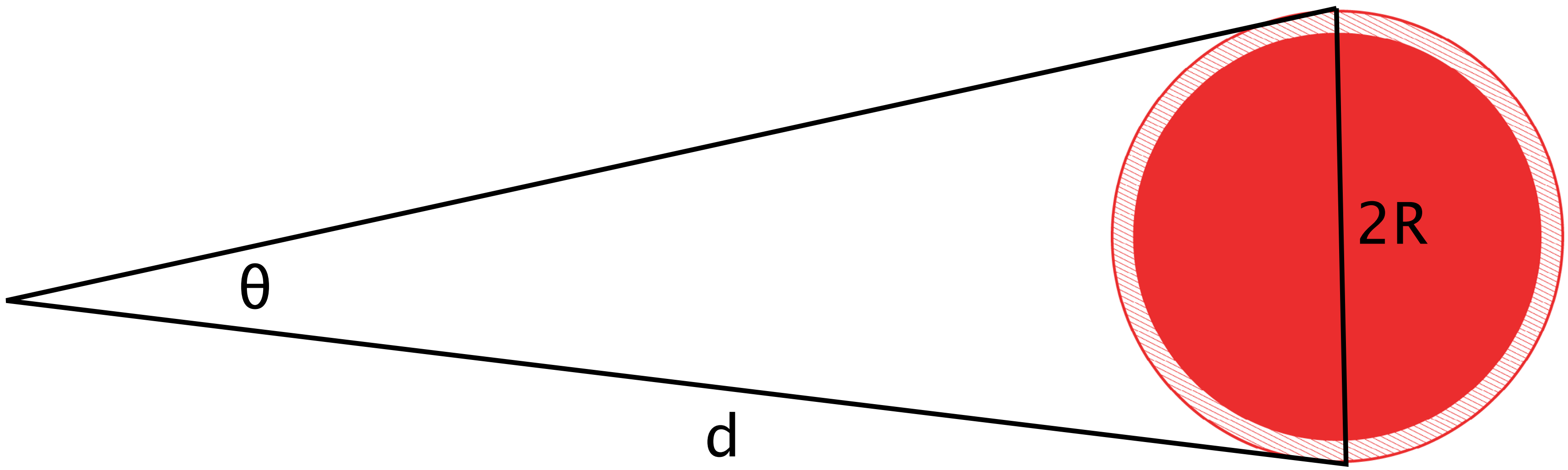

$$R = \frac{\theta d}{2}$$

$$\theta \ll 1 \text{ radian}$$

Parallax error > 1% for 4811 of the brightest (V < 6) stars

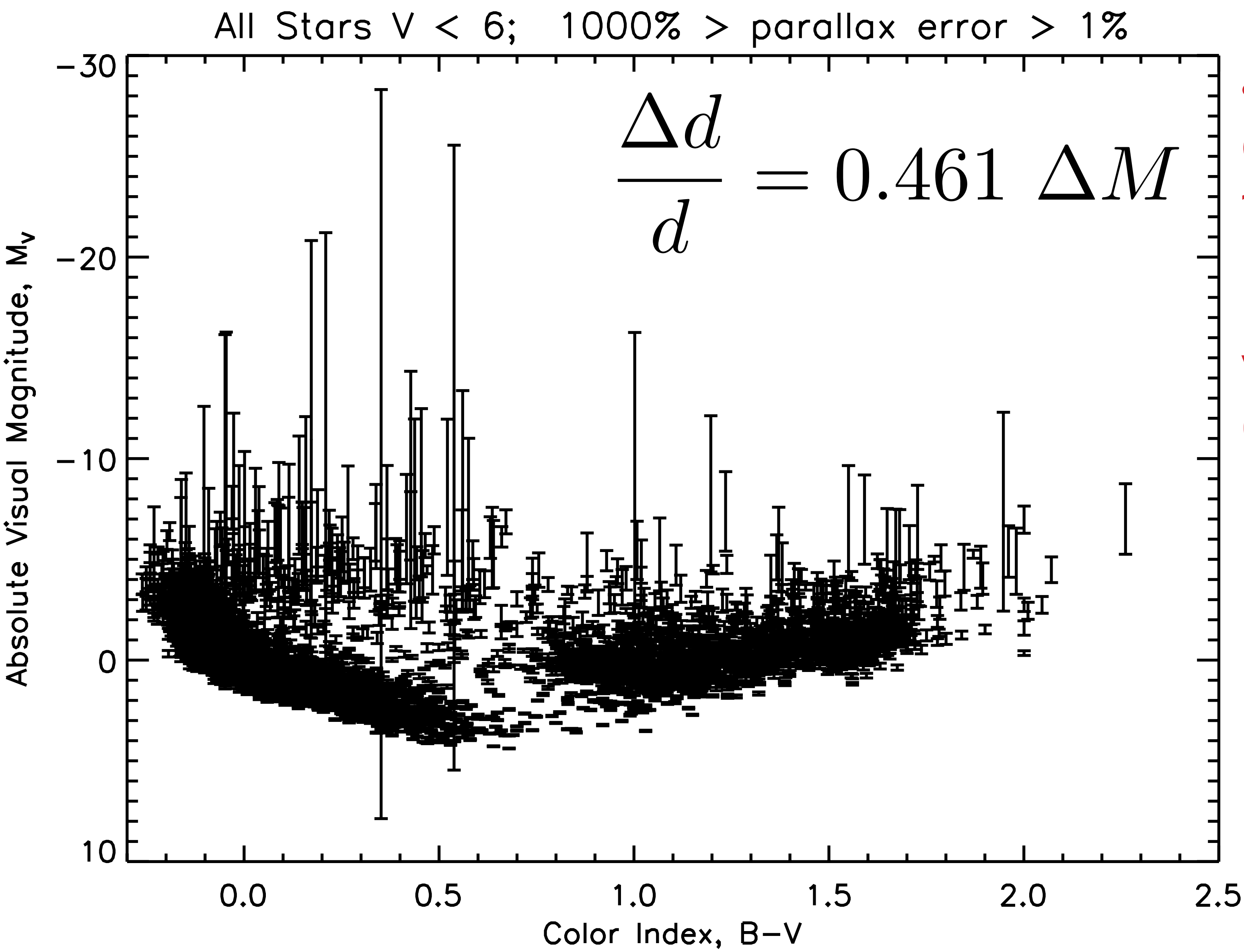

- Seven stars (V < 6) have π < 0.05 mas: HR 8154 (O8e) 32 Eri A (G8 III), V399 Car (A9Ia), θ Mus (WC+...), HR 5223 (B2IIne), HR 5680 (O8IIIp).

"Famous" stars have radius precision limited by parallax

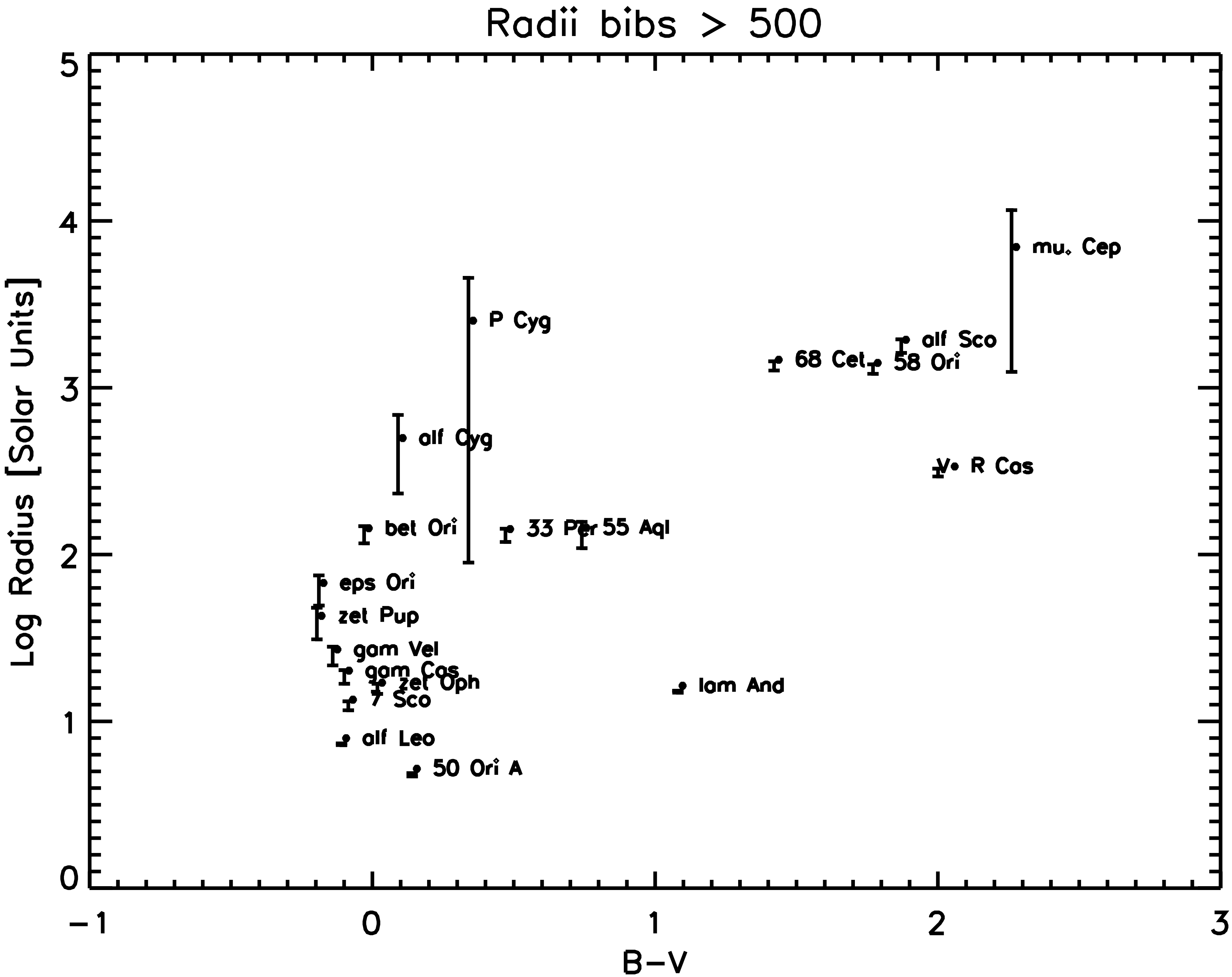

Effective Temperature from Angular Size and Flux

$$\mathrm{T_{eff}} = \left[\frac{4\mathcal{F}_0}{\sigma\theta_{\mathrm{LD}}^2}\right]^{1/4}$$

Angular Diameter (corrected for limb darkening)

Bolometric Flux (corrected for extinction)

follows from:

$$4\pi d^2 \mathcal{F}_0 = L = 4\pi R^2 \sigma \mathrm{T_{eff}^4}$$

distance

luminosity

radius

$$\mathcal{F}_0 = \frac{R^2}{d^2}\sigma \mathrm{T_{eff}^4}$$

$$\mathcal{F}_0 = \frac{\theta^2}{4}\sigma \mathrm{T_{eff}^4}$$

Effective Temperature radiates same integrated flux as the star

Effective temperature of black body radiates same integrated flux

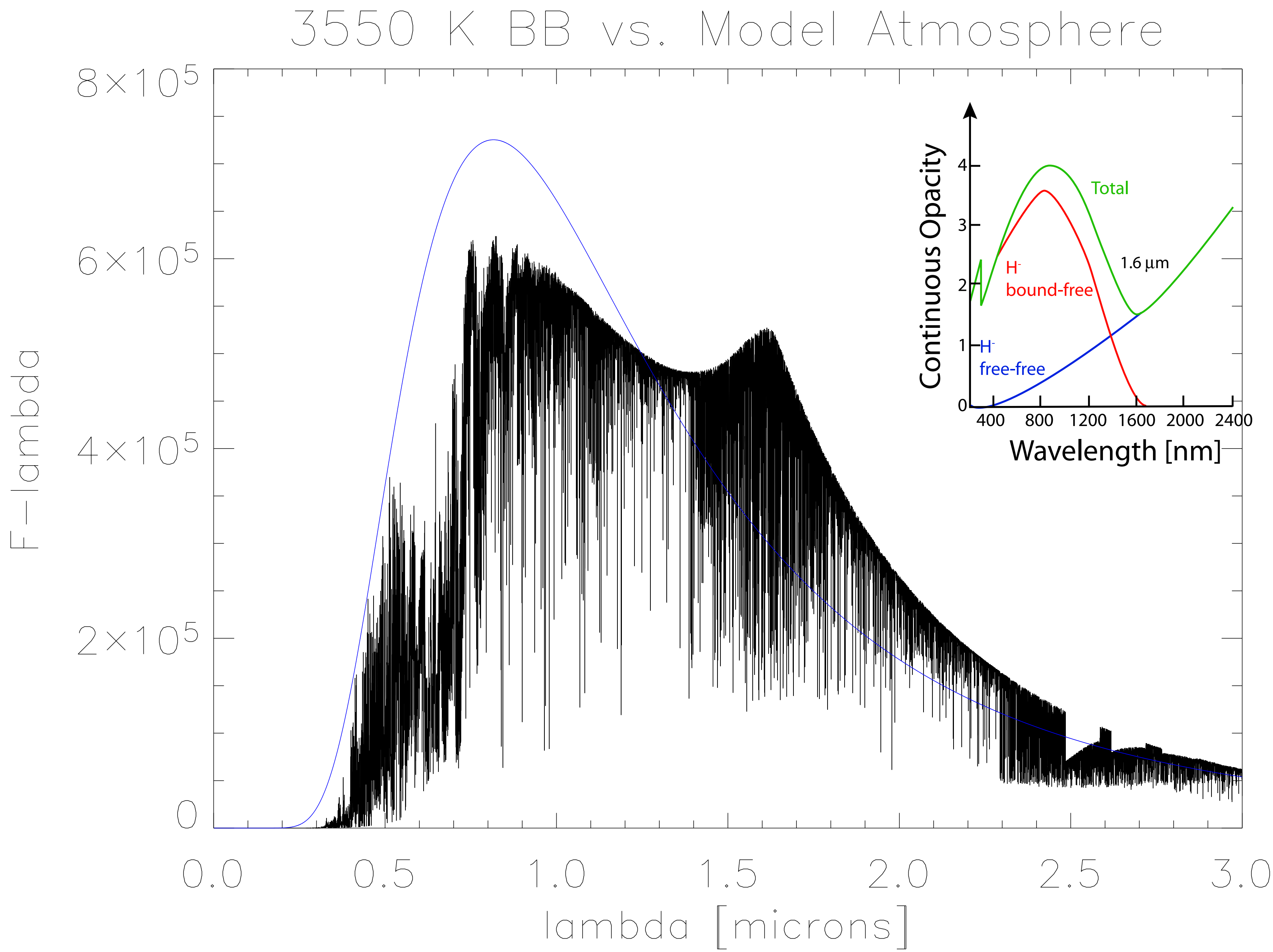

Reconstructing Temperature Structure: Spatially Resolved *Absolute* Intensities

$$T_b^{\mathrm{center}} = \frac{14388}{\lambda \ln\left[(11909/\lambda^5 I_\lambda) + 1\right]}$$

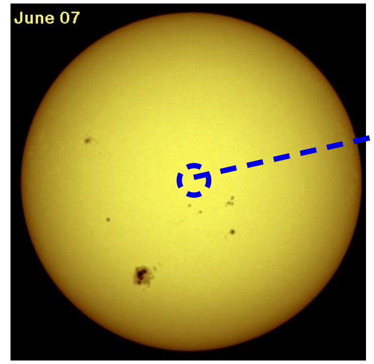

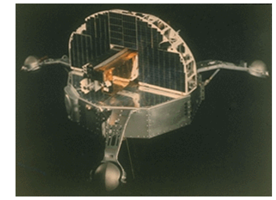

Orbiting Solar Observatory 6

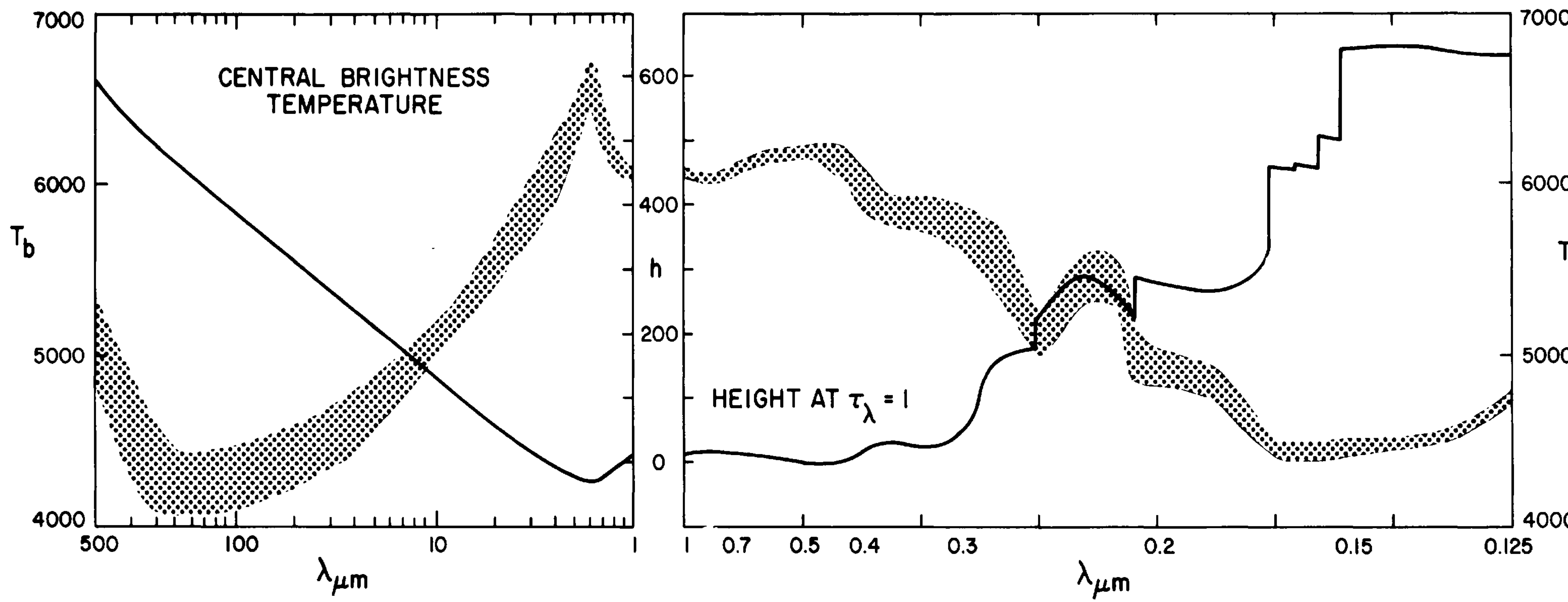

Vernazza, Avrett, & Loeser (1976) ApJS 30, 1

Limb Darkening Reveals Temperature Structure

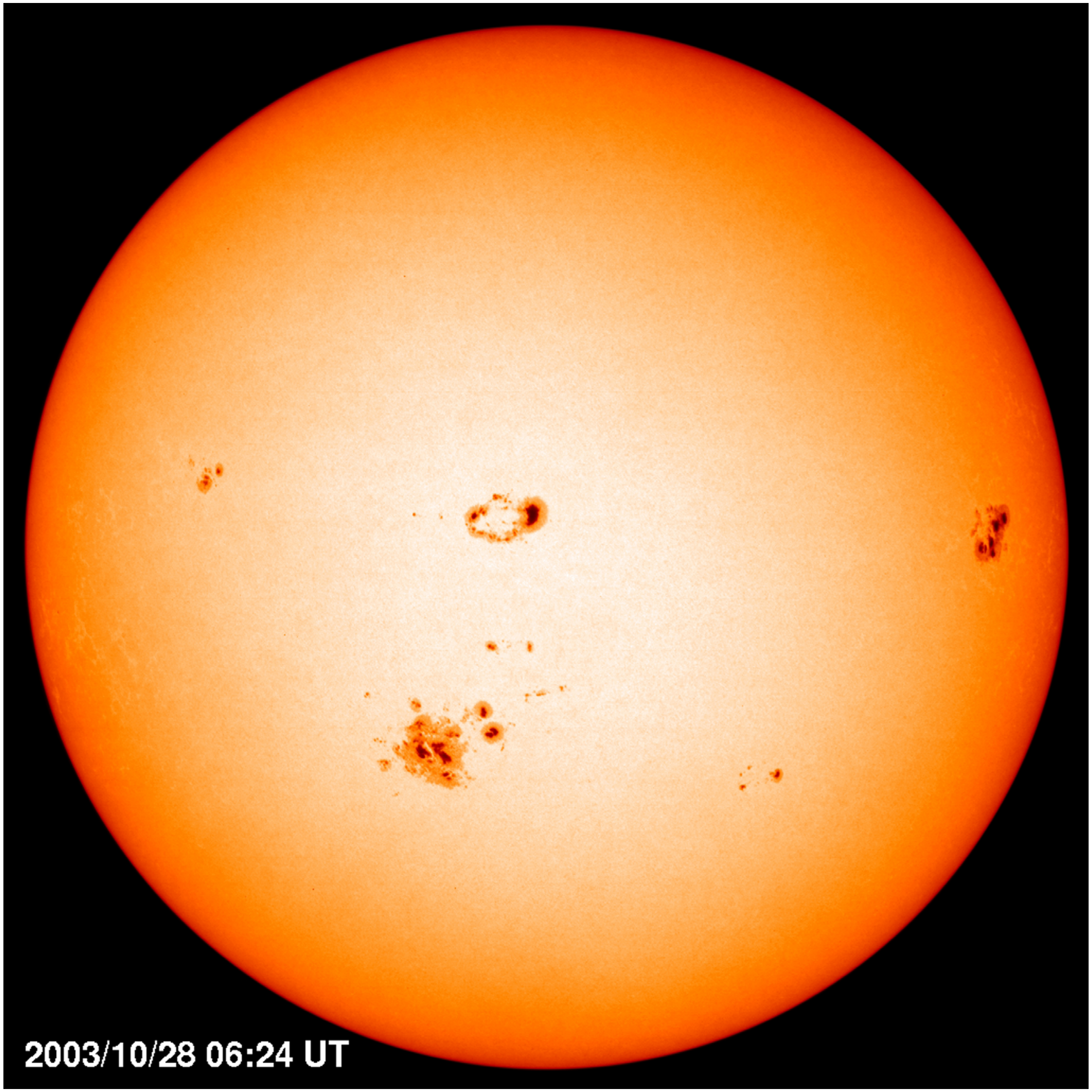

Solar and Heliospheric Observatory (SOHO), Michelson Doppler Imager (MDI)
Very narrow band Ni 6768 Å (sohowww.nascom.nasa.gov)

(a) Deeper, hotter layers are visible near the disk center

(b) Shallower, cooler layers are visible near the disk limb

isothermal atmospheres do not exhibit limb darkening

Limb Darkening Depends on Wavelength

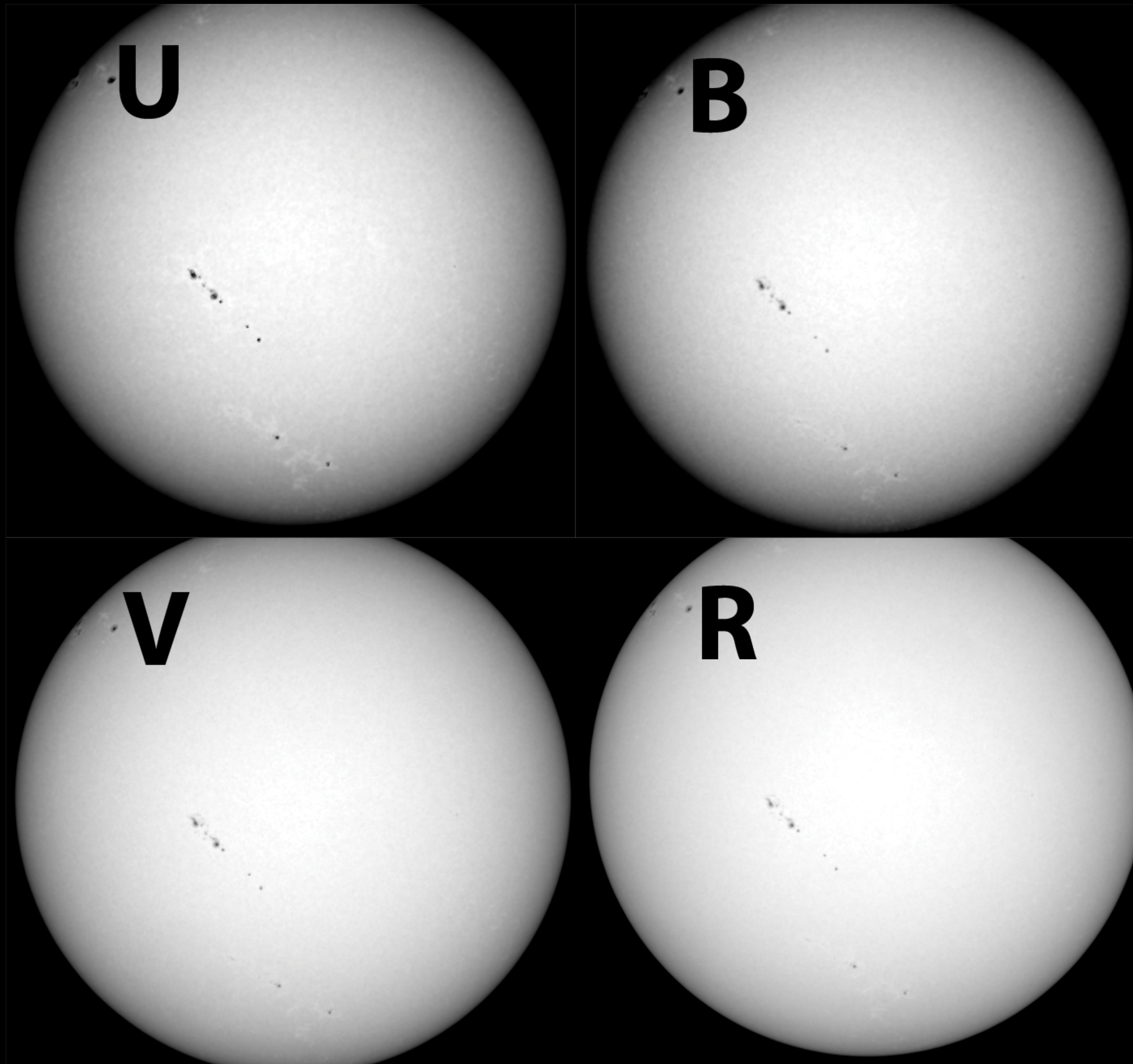

Credit: undergraduate students Edward Muller and Keily Grubaugh

Limb Darkening Depends on Wavelength

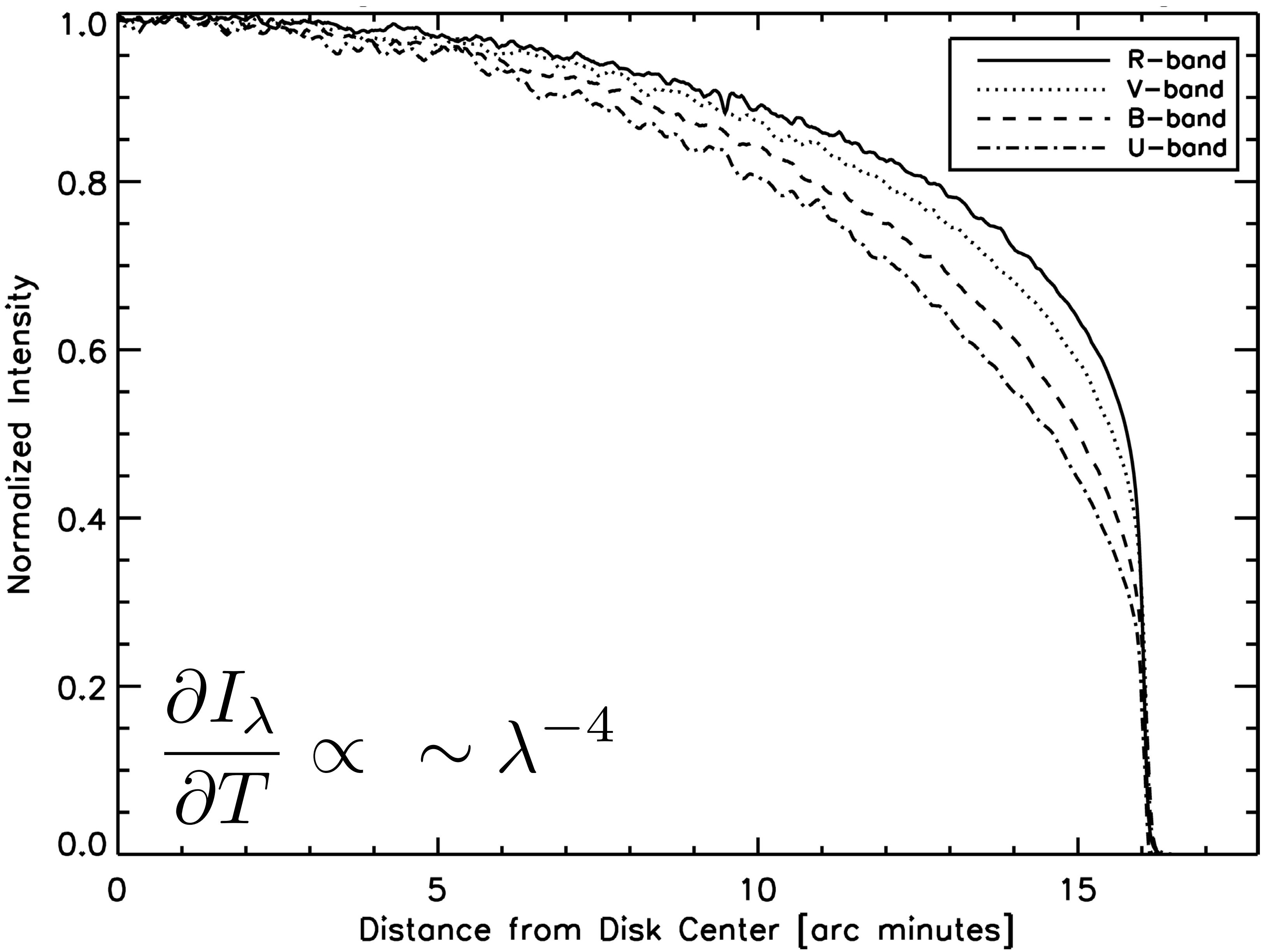

$$\frac{\partial I_\lambda}{\partial T} \propto \ \sim \lambda^{-4}$$

Credit: undergraduate students Edward Muller and Keily Grubaugh

Stellar Limb Darkening:
Geometry of a plane-parallel atmosphere

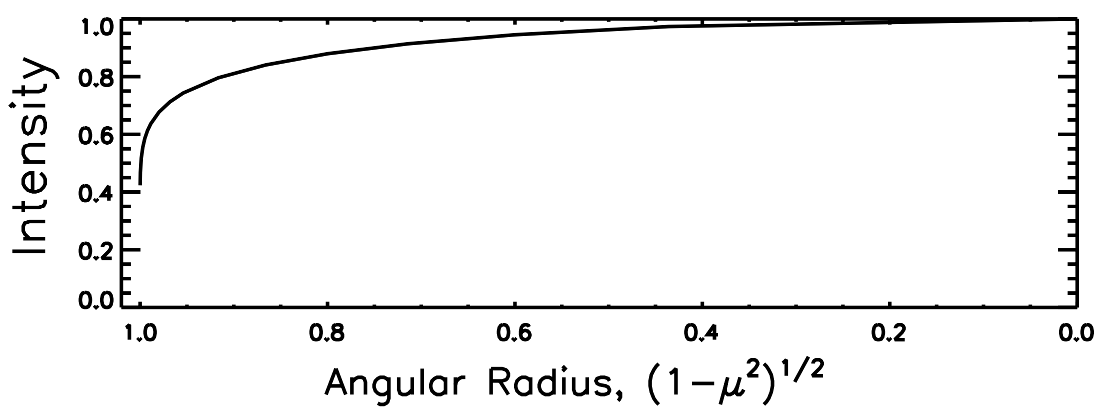

0.1% of stellar radius

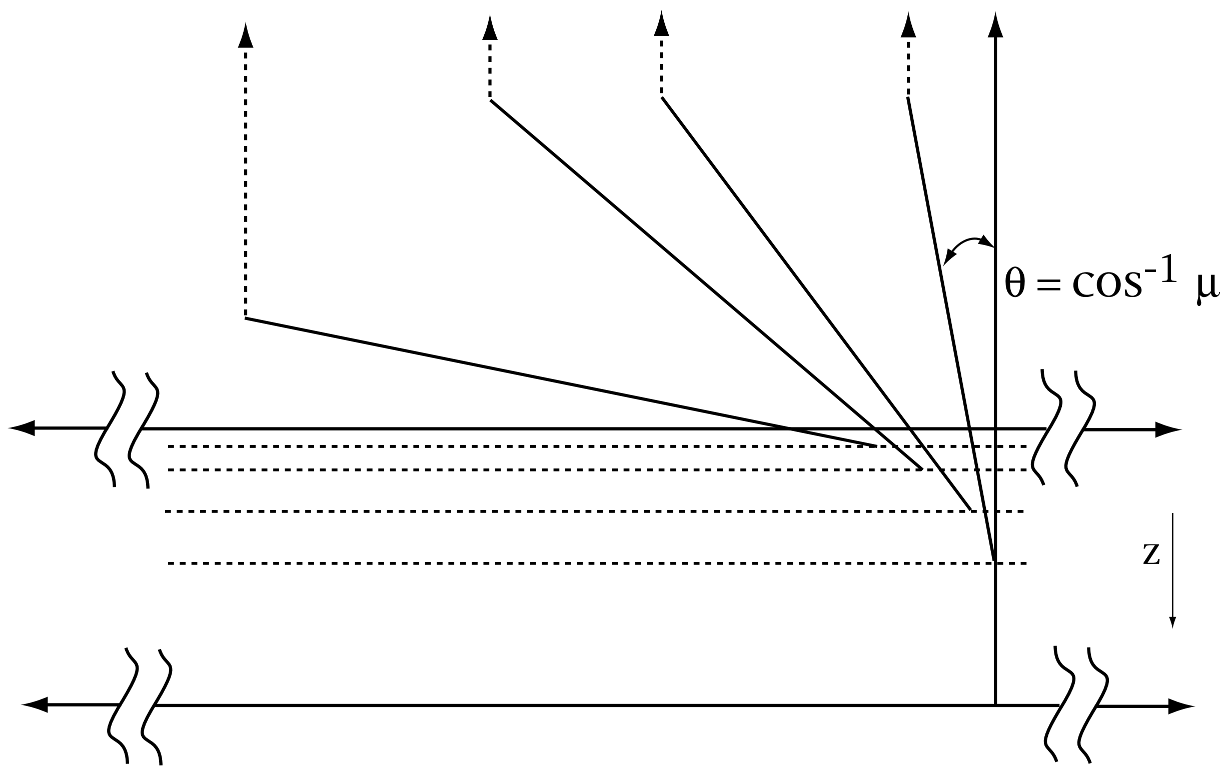

Angular Size from Interferometry

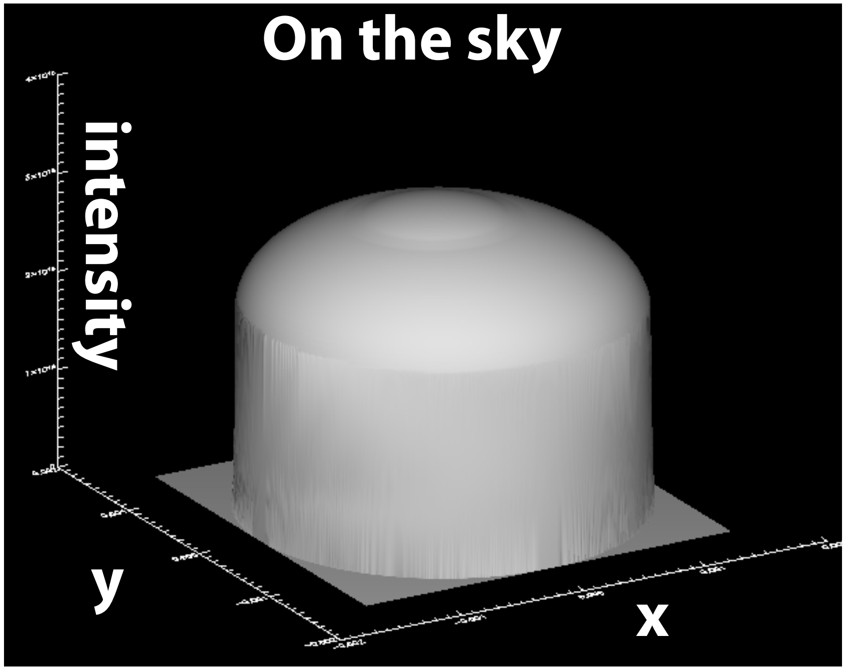

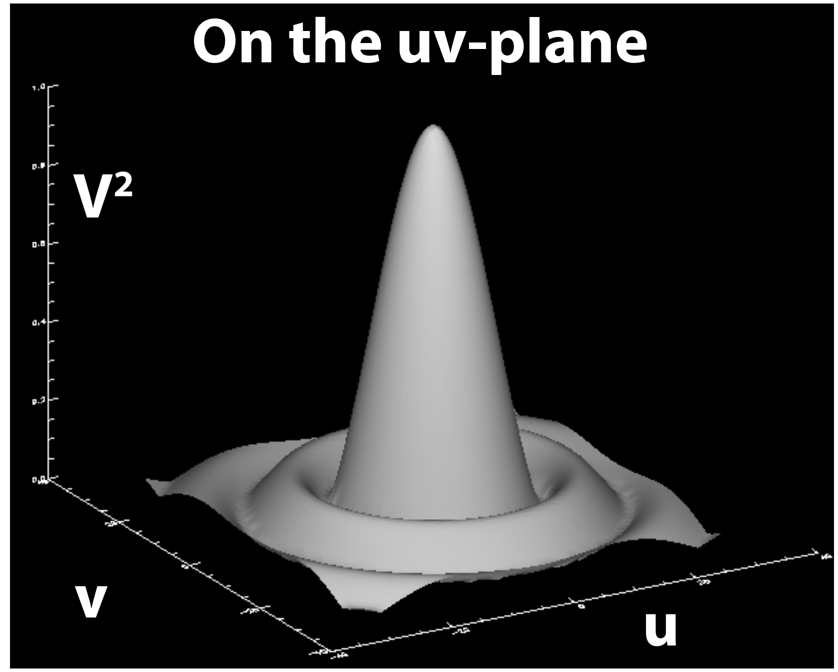

$$V_\lambda^2(u,v) = \left[\int_{-\infty}^{\infty}\int_{-\infty}^{\infty} S_\lambda I_\lambda(x,y) e^{i2\pi(u\,x+v\,y)}\,\mathrm{d}x\,\mathrm{d}y\right]^2$$

$$V^2(B,\lambda,\theta) = \left(\frac{2J_1(\pi\theta B/\lambda)}{\pi\theta B/\lambda}\right)^2 \qquad (B/\lambda)^2 = u^2 + v^2$$

How Does an Interferometer See a Single Star?

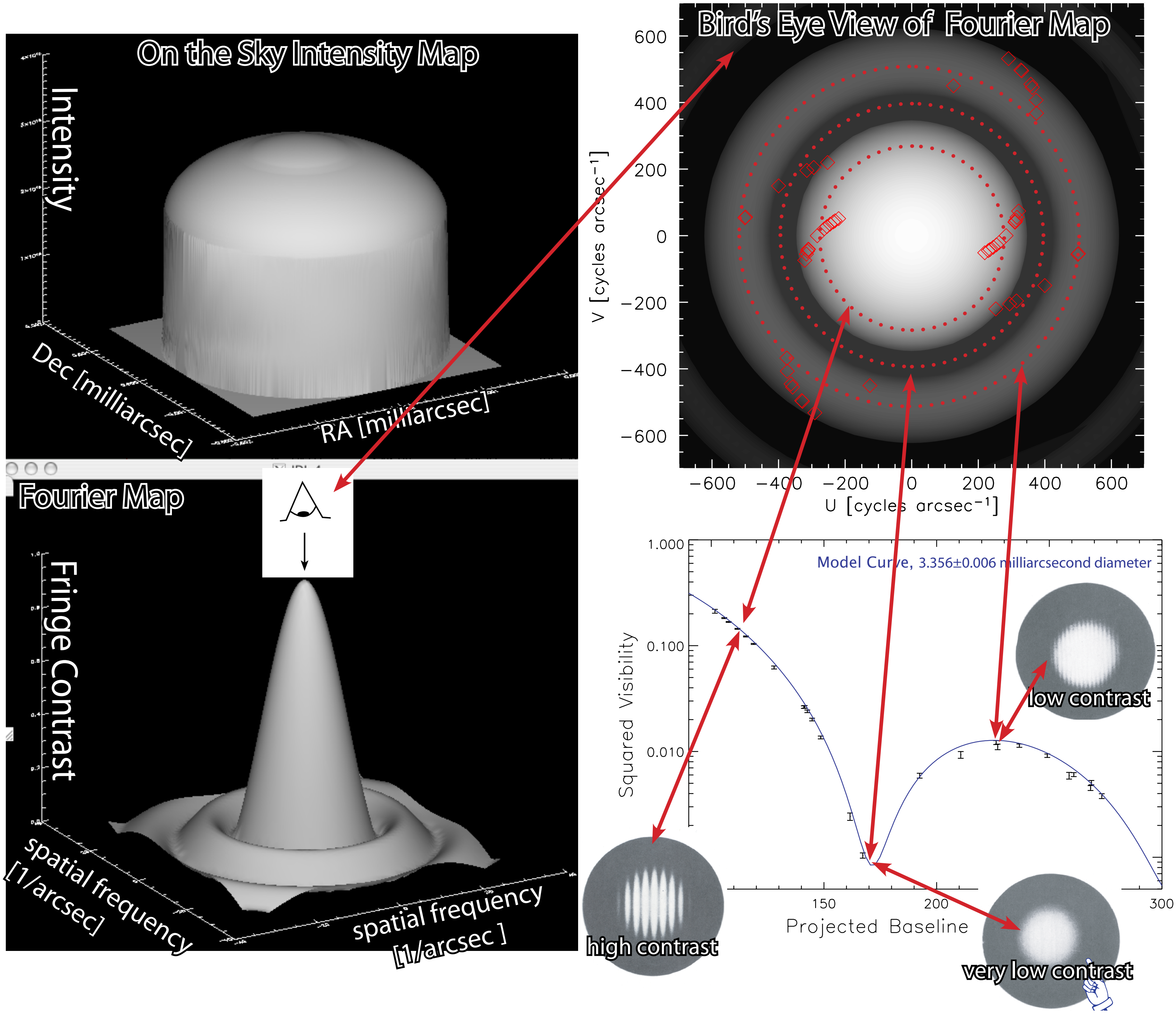

Corrections to Uniform-Disk Diameters

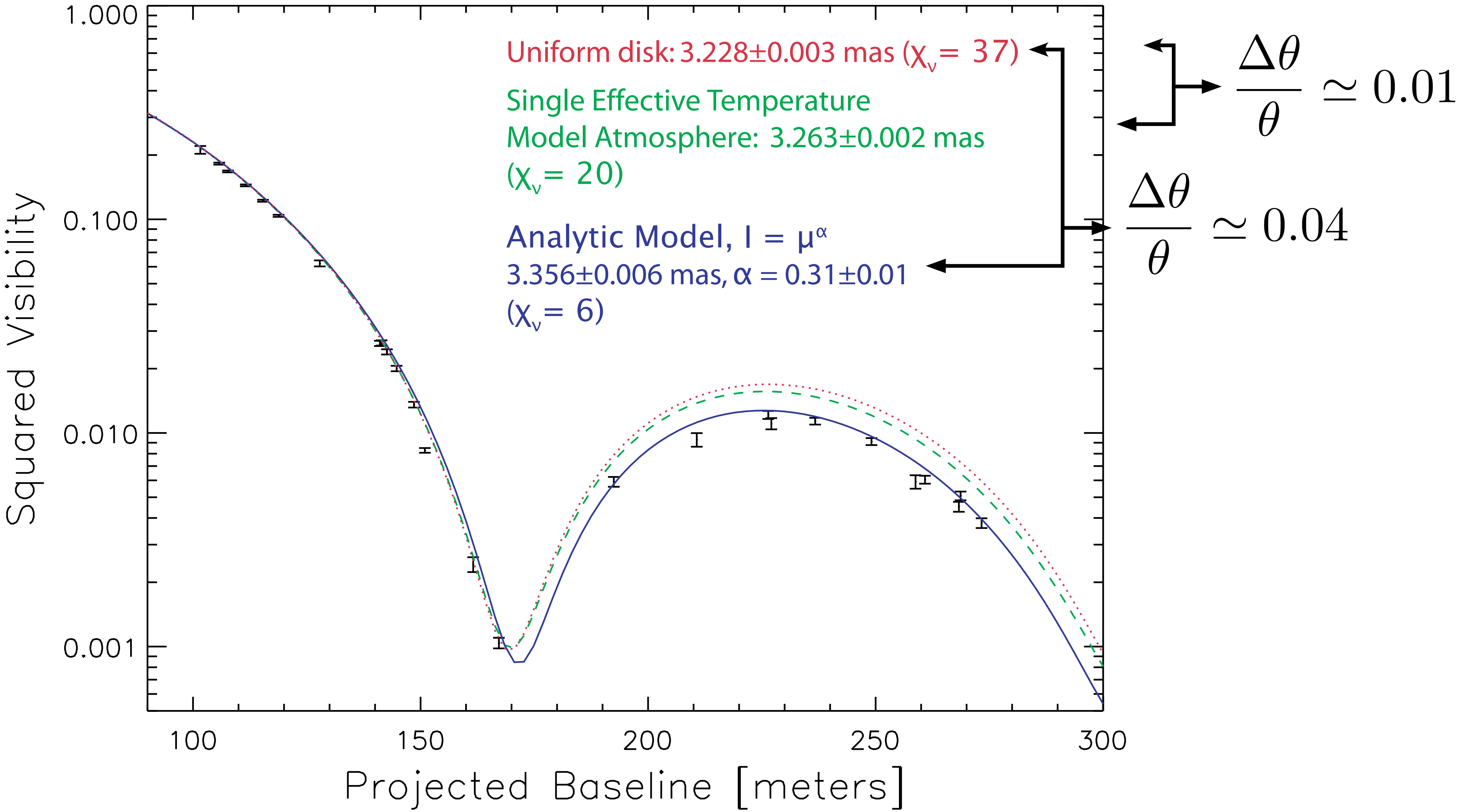

Vega (α Lyr), K-Band, CHARA/FLUOR (Aufdenberg et al. 2006, ApJ, 645, 664)

Exemplary second-lobe measurements from interferometry

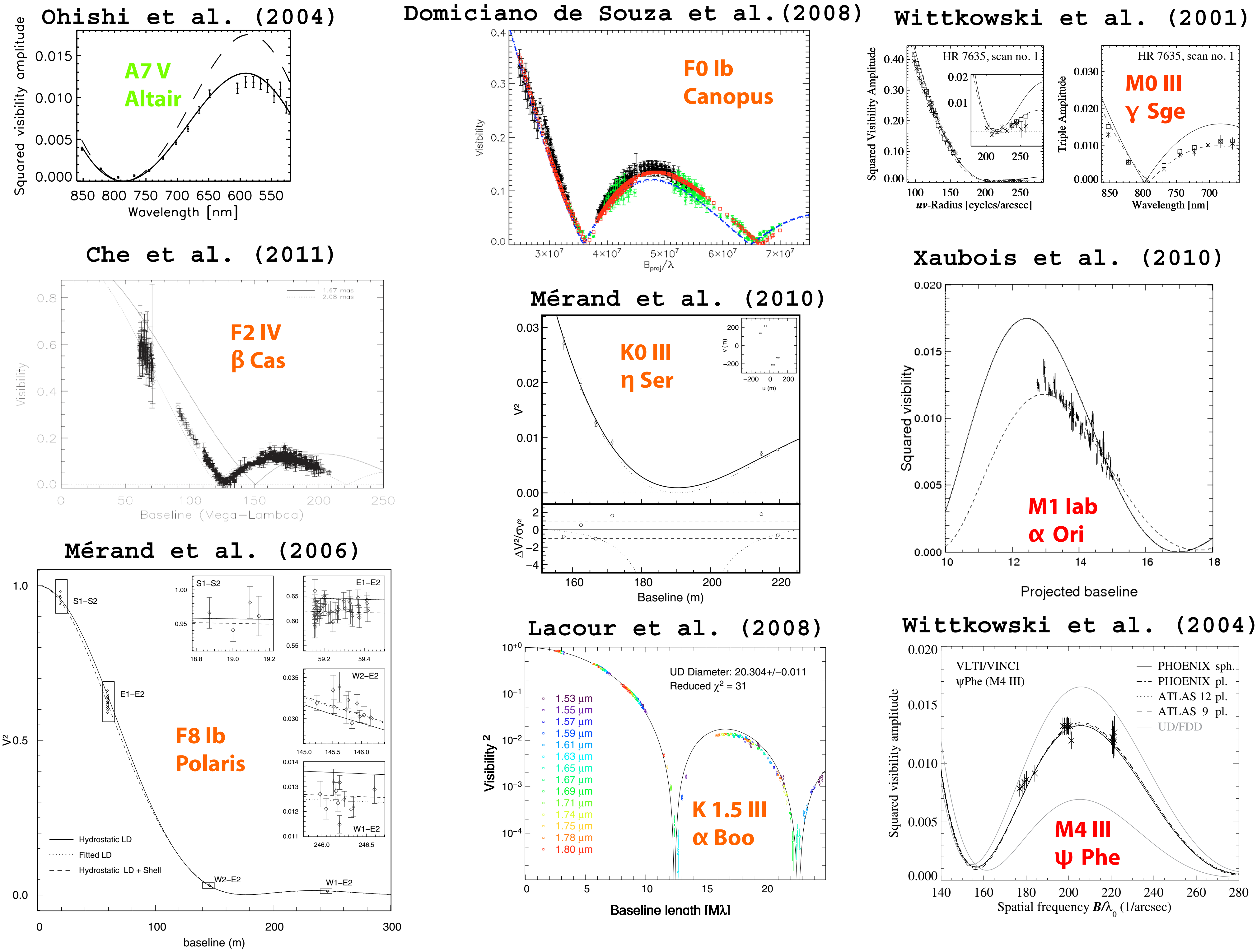

Imaging the dynamical atmosphere of the red supergiant Betelgeuse in the CO first overtone lines with VLTI/AMBER ★

K. Ohnaka[1], G. Weigelt[1], F. Millour[1,2], K.-H. Hofmann[1], T. Driebe[1,3], D. Schertl[1], A. Chelli[4], F. Massi[5], R. Petrov[2], and Ph. Stee[2]

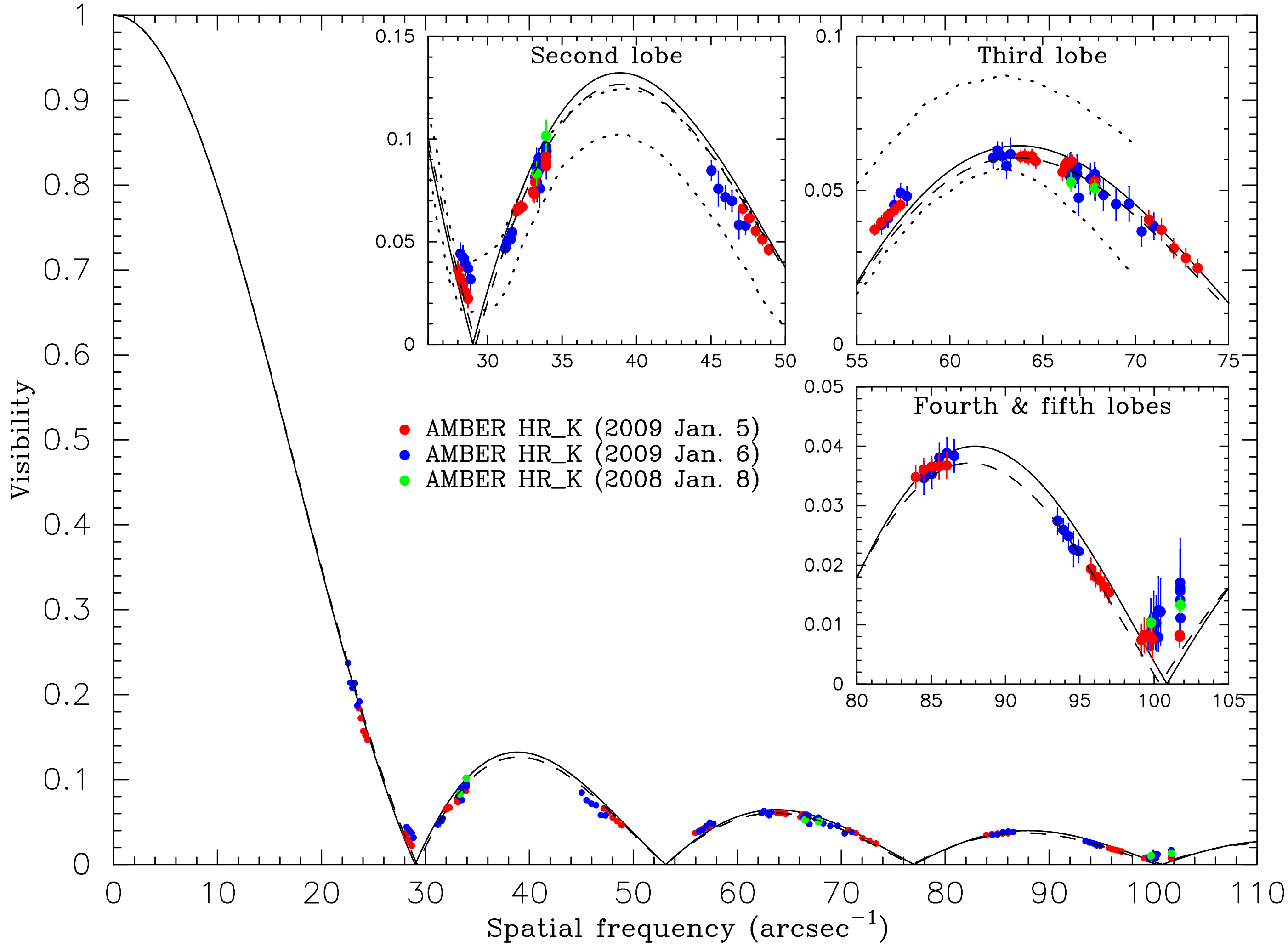

Ohnaka et al. (2011) A&A, 520, 163 [More on CO in α Ori @ 11:30!]

Second-lobe measurements from interferometry to date

M5 II	α Her	(Perrin et al. 2004)
M4.5 III	BY Boo	(Wittkowski et al. 2001)
M4 III	V416 Lac	(Wittkowski et al. 2001)
M4 III	ψ Phe	(Wittkowski et al. 2001; Wittkowski et al. 2004 (VLTI))
M1.5 III	α Cet	(Wittkowski et al. 2006) (VLTI)
M1Iab	α Ori	(Burns et al. 1997; Perrin et al. 2004; Xaubois et al. 2010, Ohnaka et al. 2011 (VLTI))
M0 III	γ Sge	(Wittkowski et al. 2001; Wittkowski et al. 2006 (VLTI))
K3 II	γ Aql	(Nordgen et al. 1999)
K2 III	α Ari	(Hajian et al. 1998)
K2 III	11 Lac	(Baines et al. 2010)
K1.5 III	α Boo	(Quirrenbach et al. 1996, Lacour et al. 2008)
K1 V	α Cen B	(Bigot et al. 2006) (VLTI)
K1 IV	γ Cep	(Baines et al. 2009)
K0 III	α Cas	(Hajian et al. 1998)
K0 III	η Ser	(Mérand et al. 2010)
F8 Ib	α UMi	(Mérand et al. 2006)
F5 Ib	α Per	(Mérand et al. 2007)
F5 IV-V	α CMi	(Aufdenberg et al. 2005)
F2 IV	β Cas	(Che et al. 2011)
F0 Ib	α Car	(Domiciano de Souza et al. 2008) (VLTI)
A7 V	α Aql	(Ohishi et al. 2004; Monnier et al. 2007)
A1 V	α CMa	(Hanbury Brown et al. 1974)
A0 V	α Lyr	(Peterson et al. 2006; Aufdenberg et al. 2006)

Tests of stellar model atmospheres by optical interferometry

VLTI/VINCI limb-darkening measurements of the M4 giant ψ Phe*

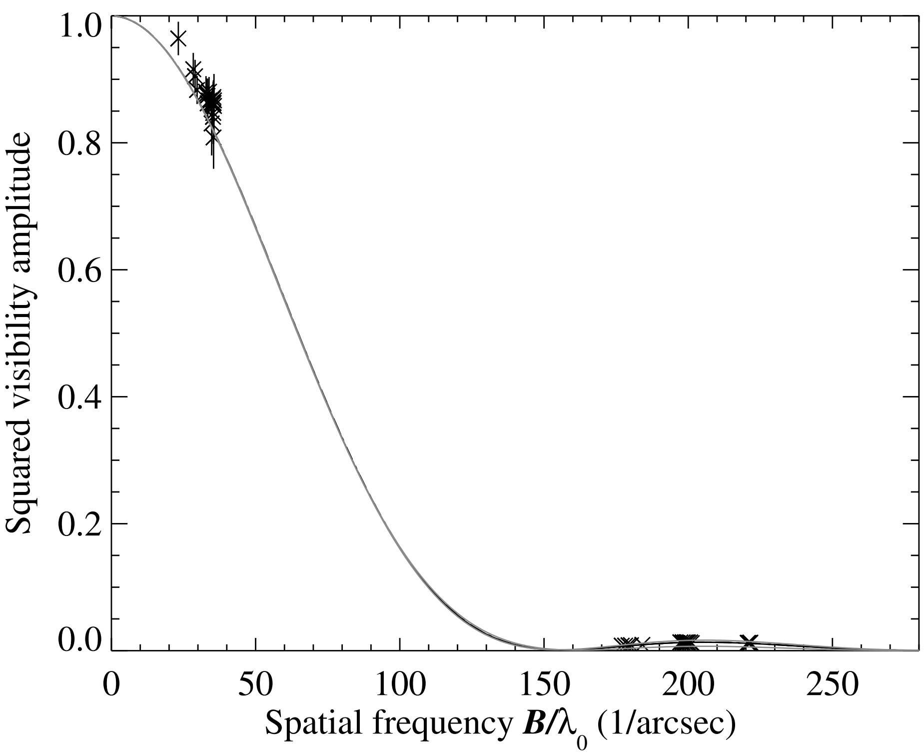

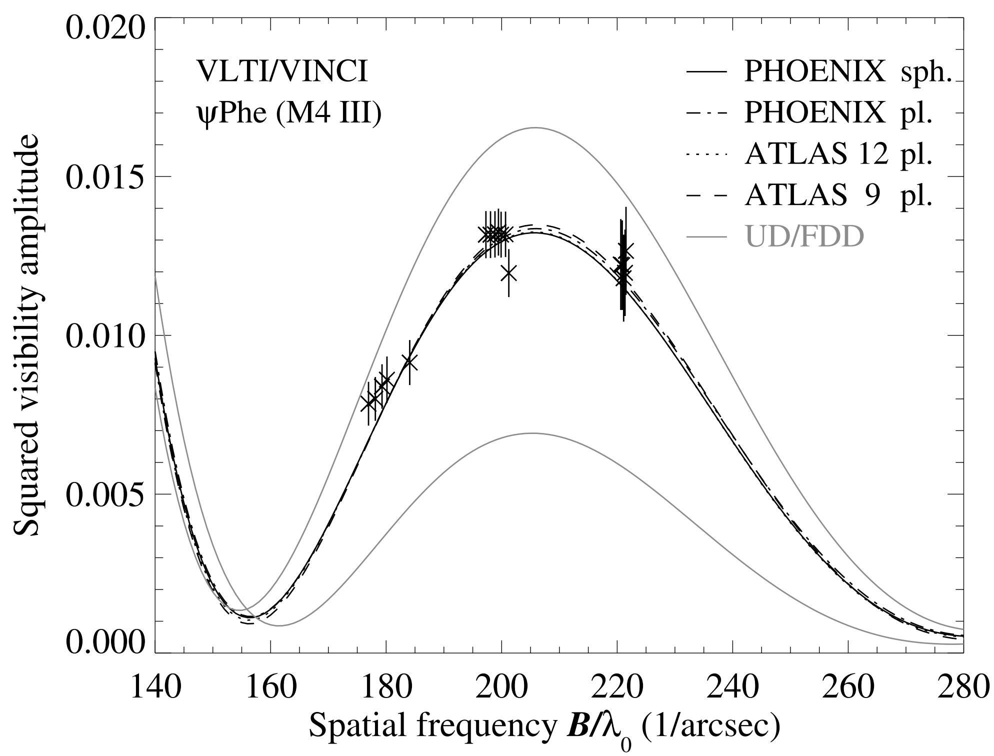

Wittkowski, Aufdenberg & Kervella (2004) A&A, 413, 711

Extracting a Diameter:
Model Geometry Matters at the 1-2% level in K-band

$T_{\rm eff}$	$\log g$	M	$C_{\rm Ross/LD}$	$\theta_{\rm LD}$	χ^2_ν	$\theta_{\rm Ross}$
Spherical PHOENIX models:						
3550	0.7	1.3	0.9388	8.664	1.80	8.13
3500	0.7	1.3	0.9394	8.663	1.81	8.14
3600	0.7	1.3	0.9381	8.665	1.79	8.13
3550	0.5	1.3	0.9218	8.814	1.79	8.12
3550	1.0	1.3	0.9577	8.504	1.79	8.14
3550	0.7	1.0	0.9302	8.739	1.80	8.13
Plane-parallel PHOENIX model:						
3550	0.7	/	1	8.168	1.72	8.17
Plane-parallel ATLAS 12 model:						
3550	0.7	/	1	8.191	1.78	8.19
Plane-parallel ATLAS 9 models:						
3500	0.5	/	1	8.244	1.74	8.24
3500	1.0	/	1	8.243	1.73	8.24
3750	0.5	/	1	8.227	1.71	8.23
3750	1.0	/	1	8.228	1.71	8.23

VLTI/VINCI K-band

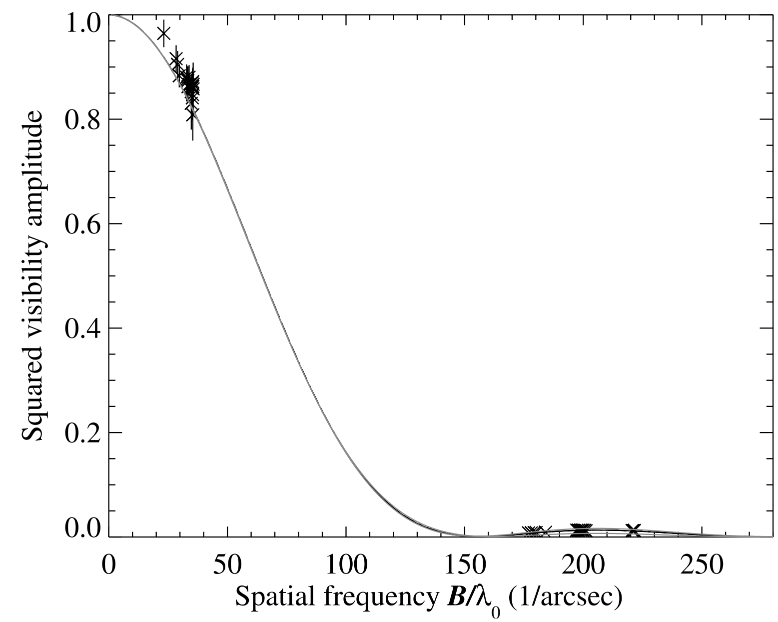

$$\frac{\Delta\theta}{\theta} \simeq 0.015$$

ψ Phe: Wittkowski, Aufdenberg & Kervella (2004) A&A, 413, 711

Spherical Atmospheres: same gravity, different mass

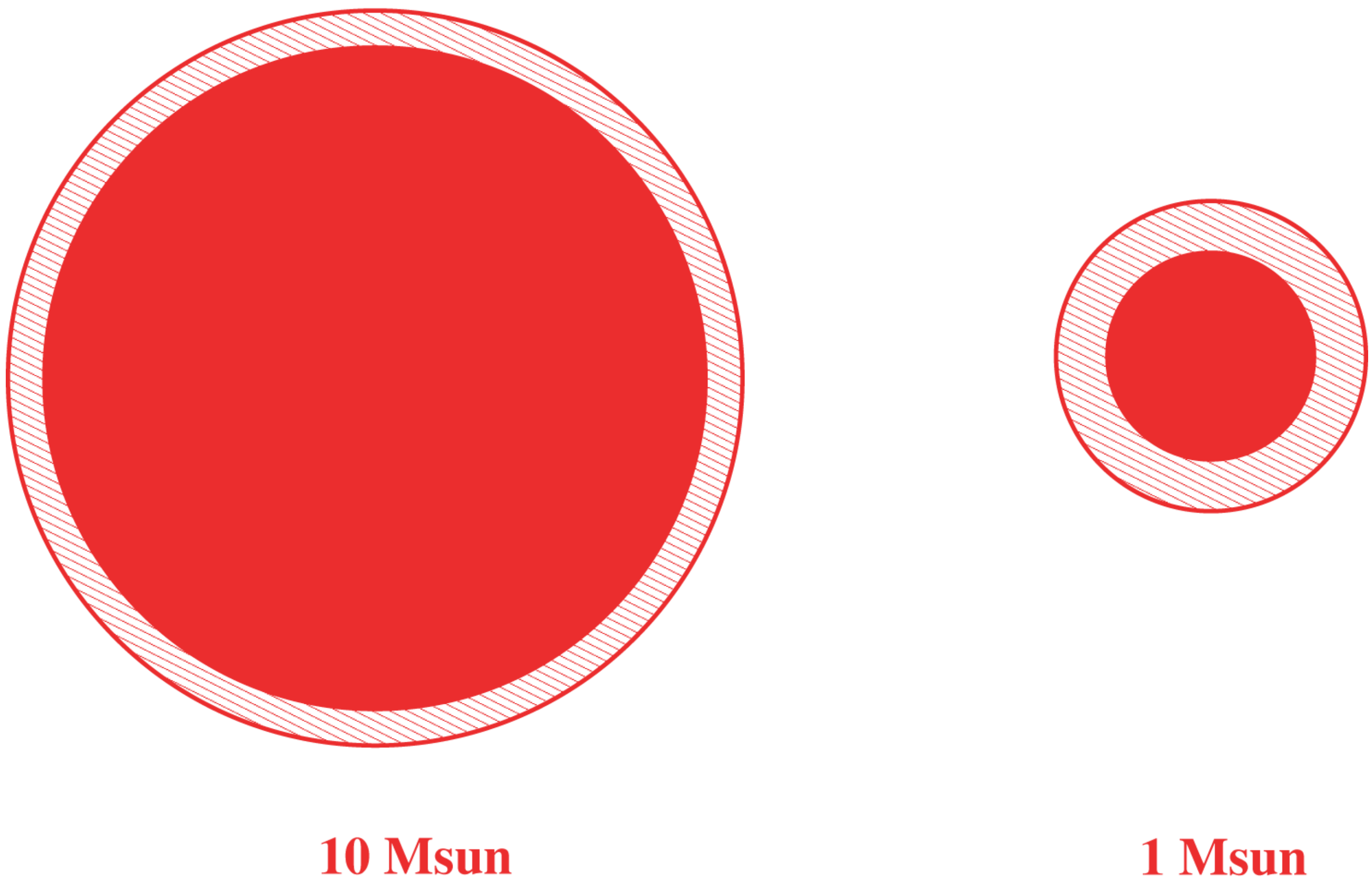

Two stars: same T_{eff} and log(g), different Mass

Spherical Geometry and Atmospheric Extension

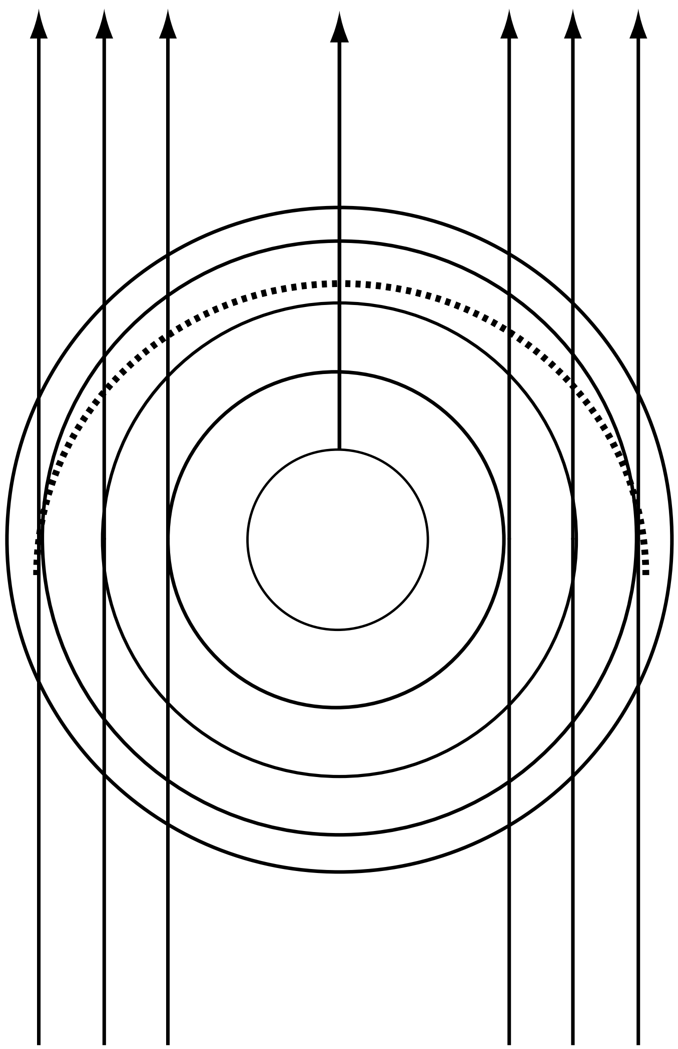

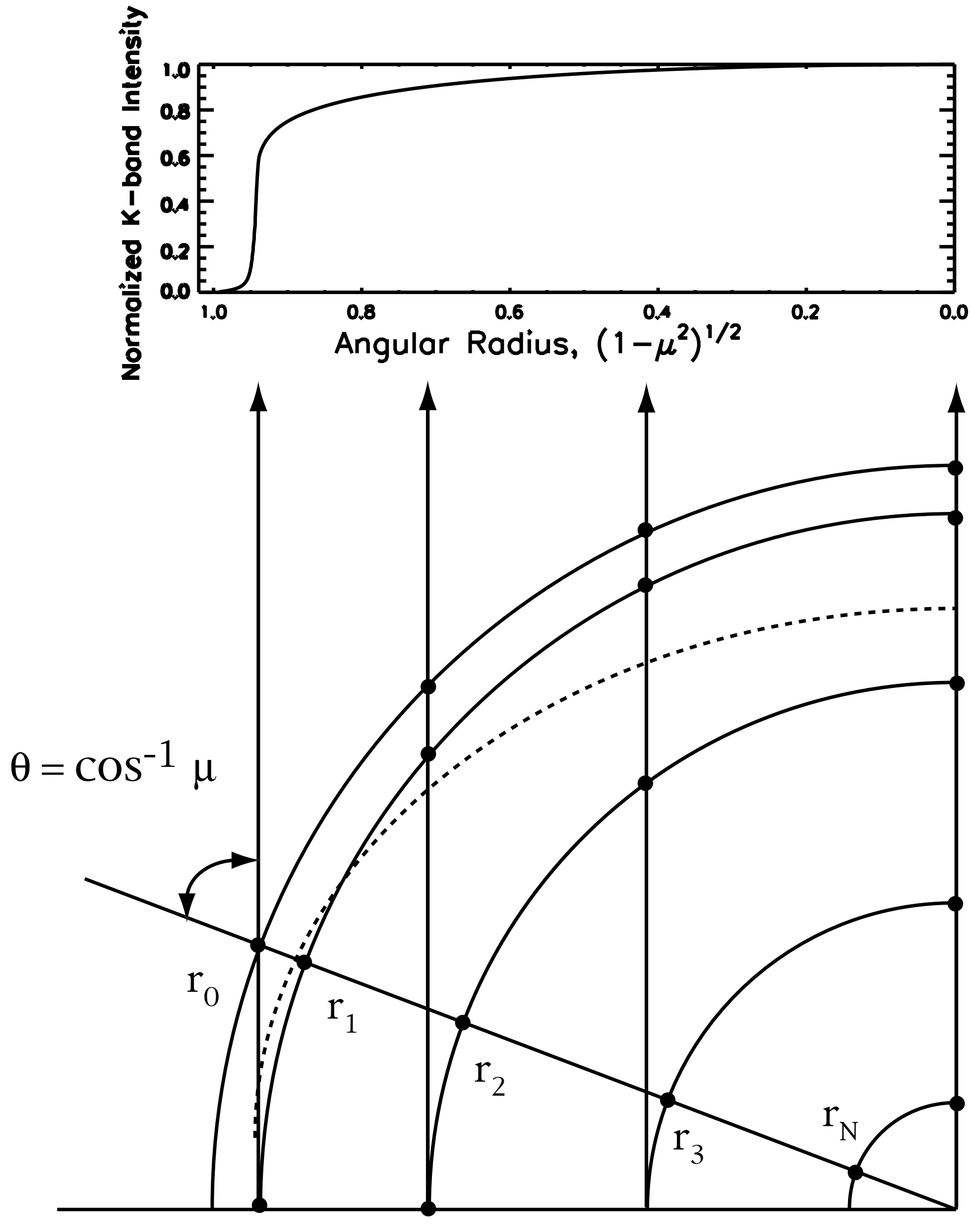

Tests of stellar model atmospheres by optical interferometry

III. NPOI and VINCI interferometry of the M0 giant γ Sagittae covering 0.5–2.2 μm[⋆,⋆⋆]

M. Wittkowski[1], C. A. Hummel[2], J. P. Aufdenberg[3], and V. Roccatagliata[4]

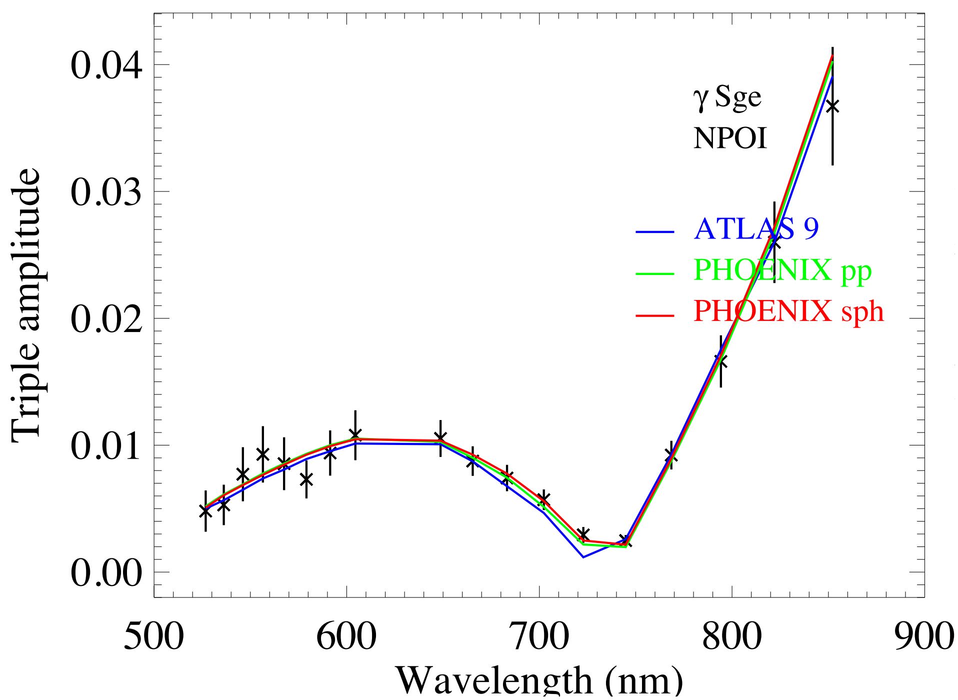

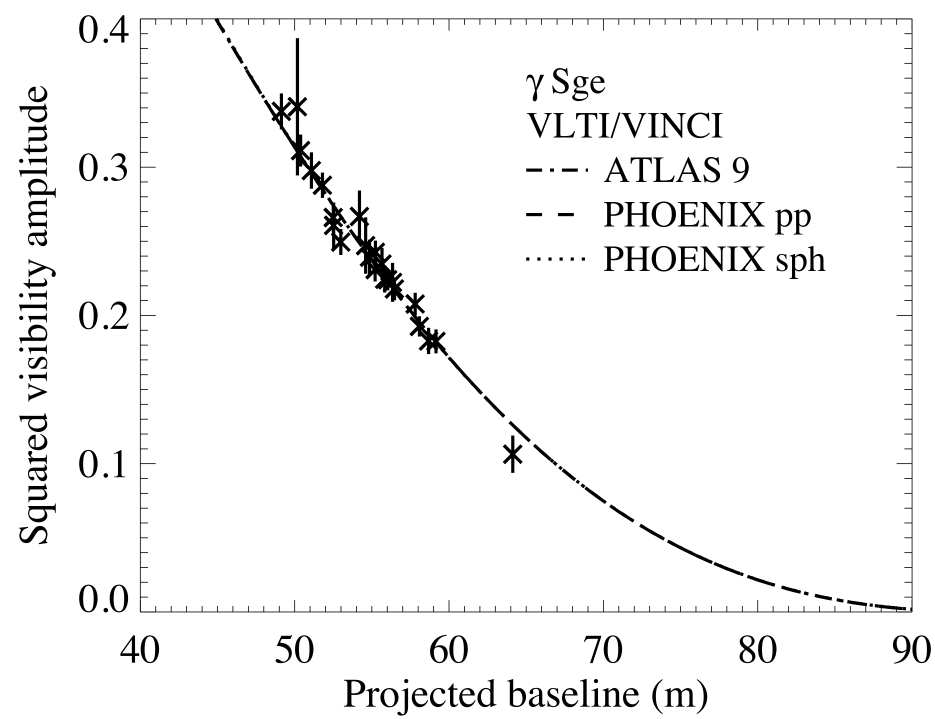

Wittkowski et al. (2006) A&A, 460, 843

Spherical Model Yields Consistent Angular Diameter Across Optical/Near-IR for γ Sge (M0 III)

Model atmosphere	NPOI (526 nm to 852 nm)	VLTI/VINCI (2190 nm)
ATLAS 9, plane-parallel, $T_{\rm eff}$ = 3750 K, log g = 1.0	$\Theta_{\rm LD}$ = 6.18 ± 0.06 mas χ^2_ν = 2.2	$\Theta_{\rm LD}$ = 6.05 ± 0.02 mas χ^2_ν = 0.6
PHOENIX, plane-parallel, $T_{\rm eff}$ = 3750 K, log g = 1.0	$\Theta_{\rm LD}$ = 6.11 ± 0.06 mas χ^2_ν = 2.3	$\Theta_{\rm LD}$ = 6.05 ± 0.02 mas χ^2_ν = 0.6
PHOENIX, spherical, $T_{\rm eff}$ = 3750 K, log g = 1.0, $\boxed{M = 1.3\,M_\odot}$	$\Theta_{\rm LD}$ = 6.30 ± 0.06 mas χ^2_ν = 2.4 $\Theta_{\rm Ross}$ = 6.02 ± 0.06 mas	$\Theta_{\rm LD}$ = 6.30 ± 0.02 mas χ^2_ν = 0.6 $\Theta_{\rm Ross}$ = 6.02 ± 0.02 mas

All atmosphere models have: $T_{\rm eff}$ = 3750 K, log(g) = 1.0
but different geometries

Wittkowski et al. (2006) A&A, 460, 843

The limb darkening of α Centauri B

Matching 3D hydrodynamical models with interferometric measurements

L. Bigot[1], P. Kervella[2], F. Thévenin[1], and D. Ségransan[3]

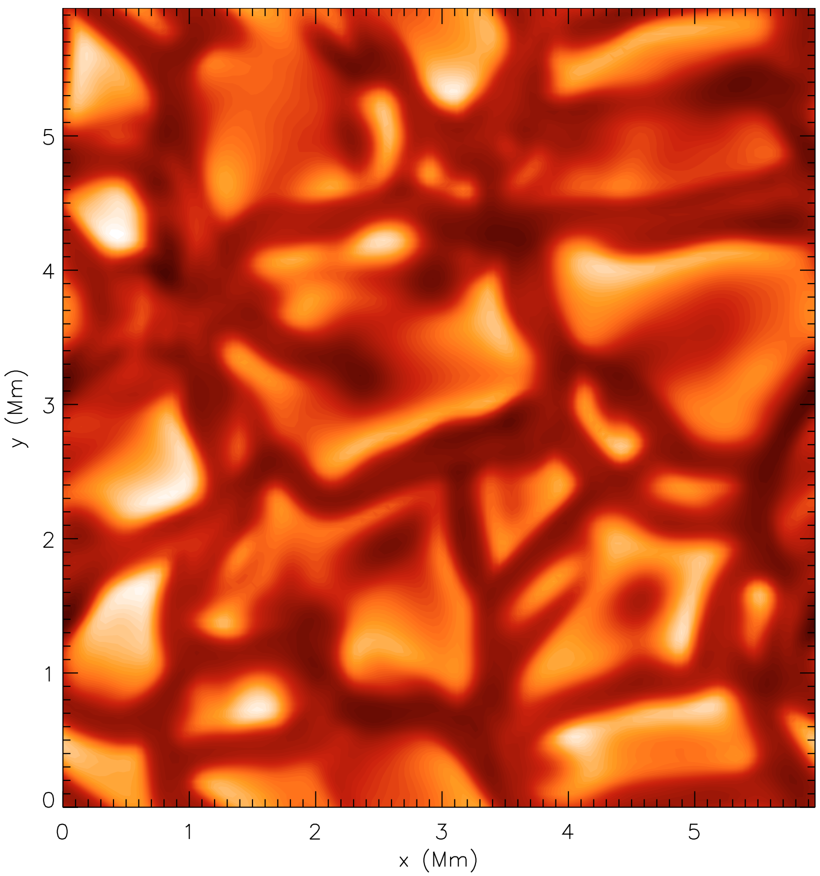

3D RHD Surface

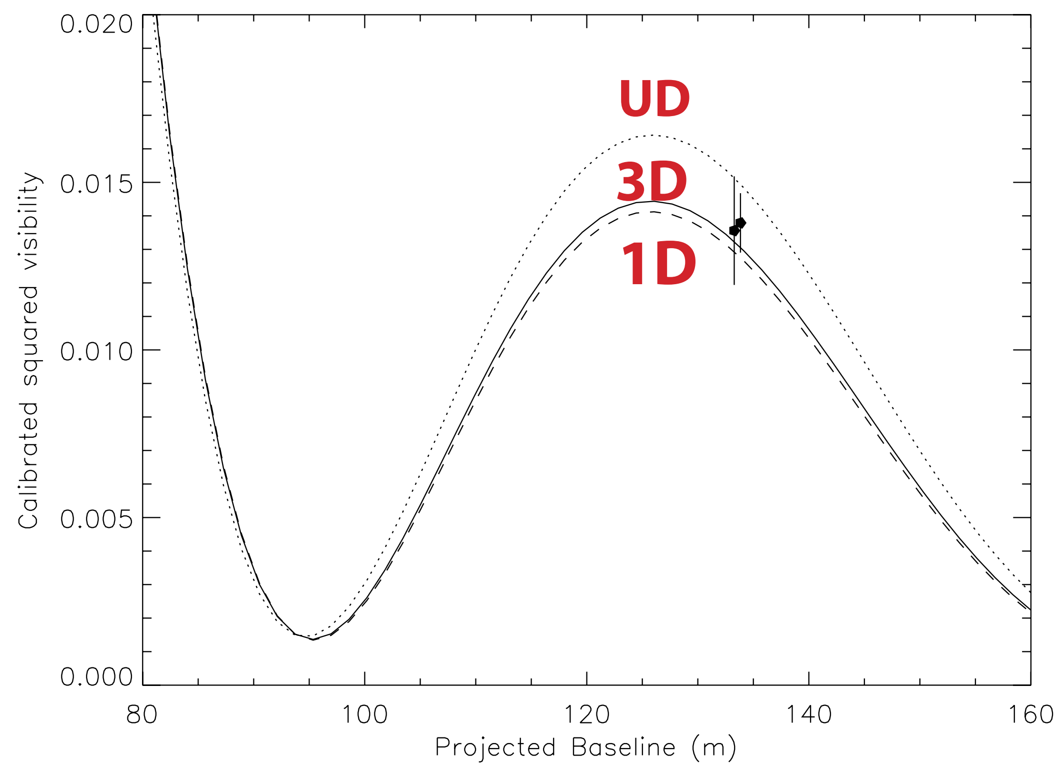

Bigot et al. (2006) A&A, 446, 635

3-D Radiative Hydrodynamic vs. 1-D Center-to-Limb Variations

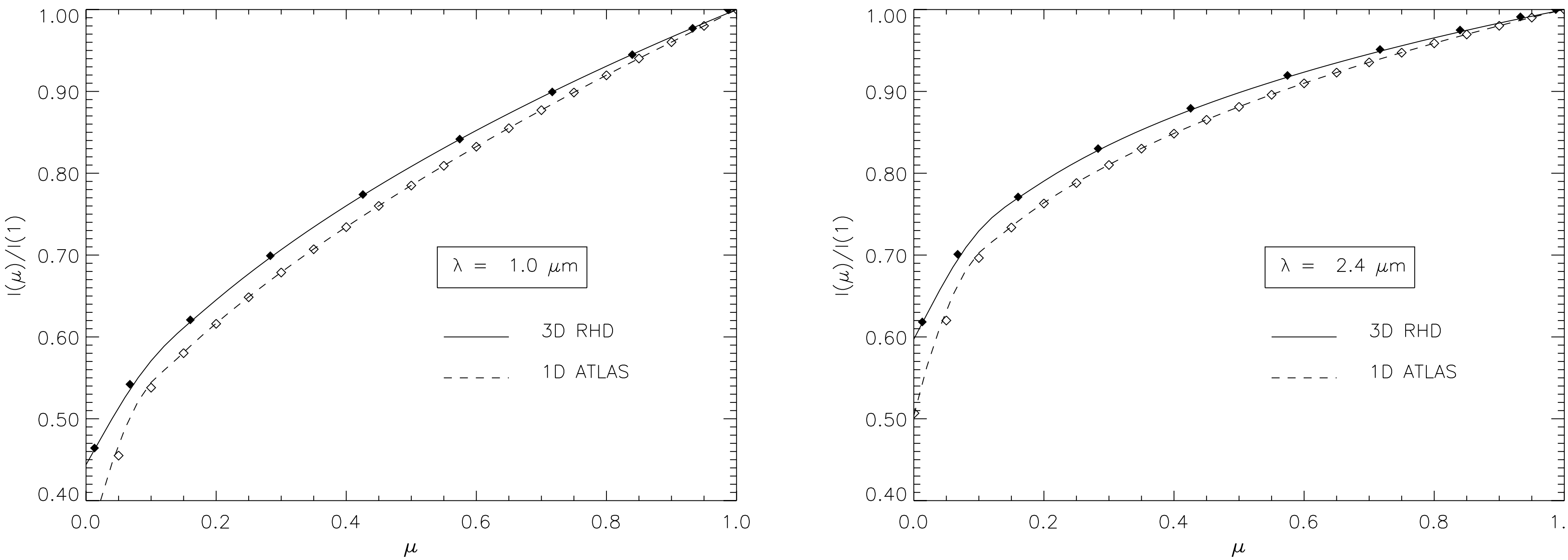

- **Limb darkening weaker at longer wavelengths**
- **3D RHD models less limb darkened than (standard) 1-D models**

Bigot et al. (2006) A&A, 446, 635

ON THE LIMB DARKENING, SPECTRAL ENERGY DISTRIBUTION, AND TEMPERATURE STRUCTURE OF PROCYON

J. P. Aufdenberg[1]
National Optical Astronomy Observatory, 950 North Cherry Avenue, Tucson, AZ 85719

H.-G. Ludwig
Lund Observatory, Lund University, Box 43, 22100 Lund, Sweden

AND

P. Kervella
LESIA, UMR 8109, Observatoire de Paris-Meudon, 5 place Jules Janssen, 92195 Meudon Cedex, France

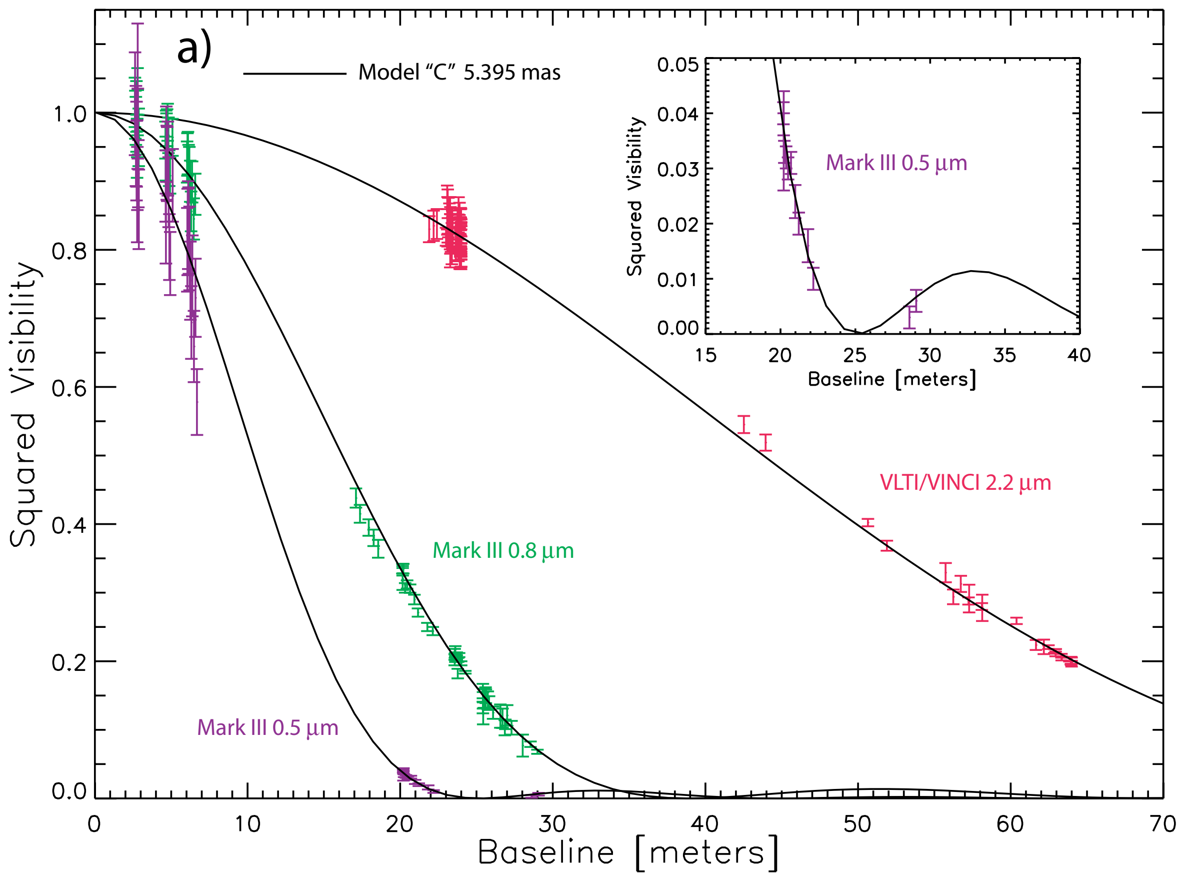

Procyon = α CMa (F5 IV-V)

- **Different UD angular diameters at 500 nm, 800nm, 2.2 µm reveal limb darkening**
- **LImb darkening most sensitive to temperature structure at shortest wavelength**

Aufdenberg, Ludwig & Kervella (2005) ApJ, 633, 424

Procyon: Convection Effects on Limb Darkening

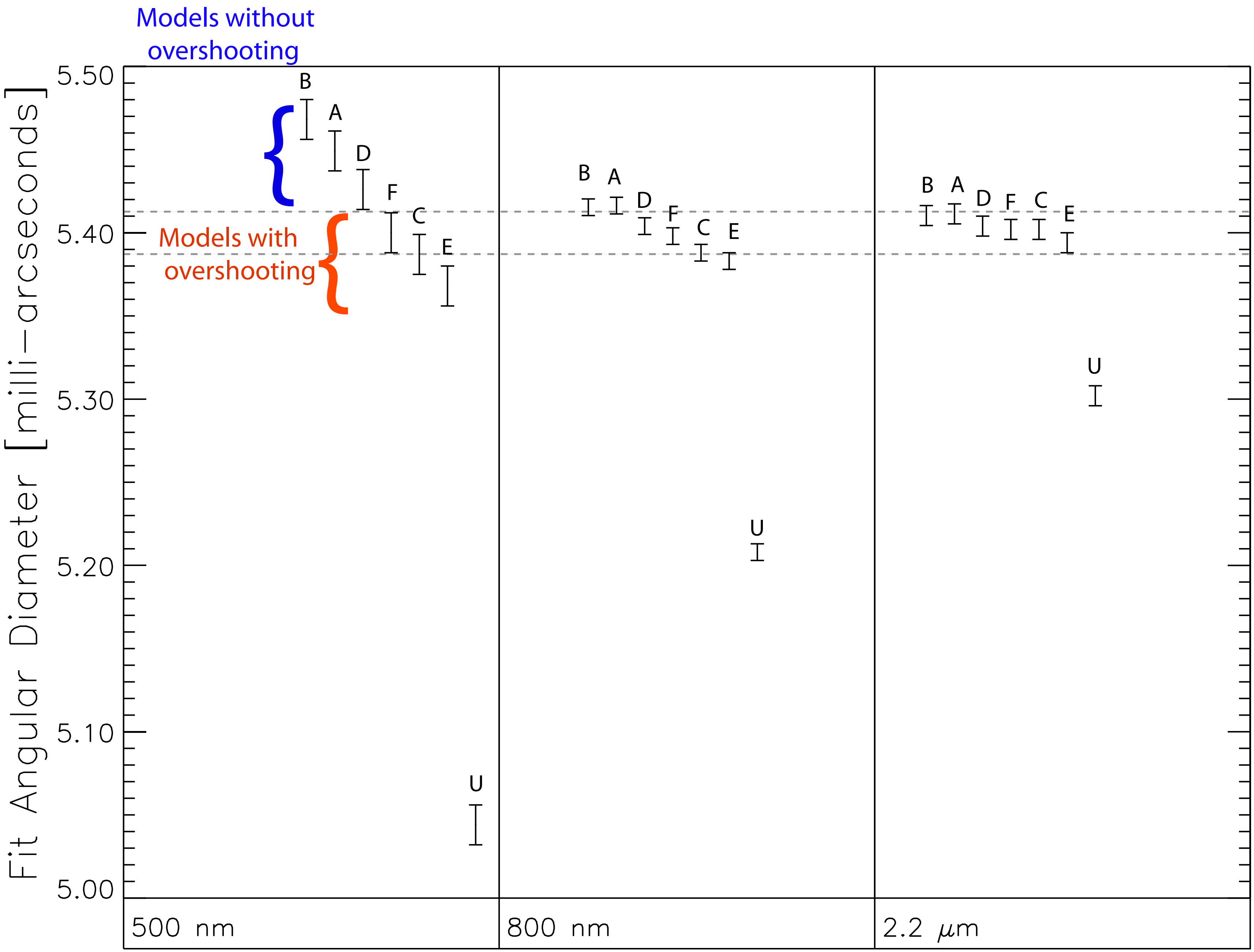

B: PHOENIX "B"
A: PHOENIX "A"
D: ATLAS "D"
F: ATLAS "F"
C: CO^5BOLD + PHOENIX
E: ATLAS "E"
U: Uniform Disk

All atmosphere models have:

T_{eff} = 6530 K
log(g) = 3.95

but different convection treatments

Aufdenberg, Ludwig & Kervella (2005) ApJ, 633, 424

Limb Darkening and Convection in the Sun

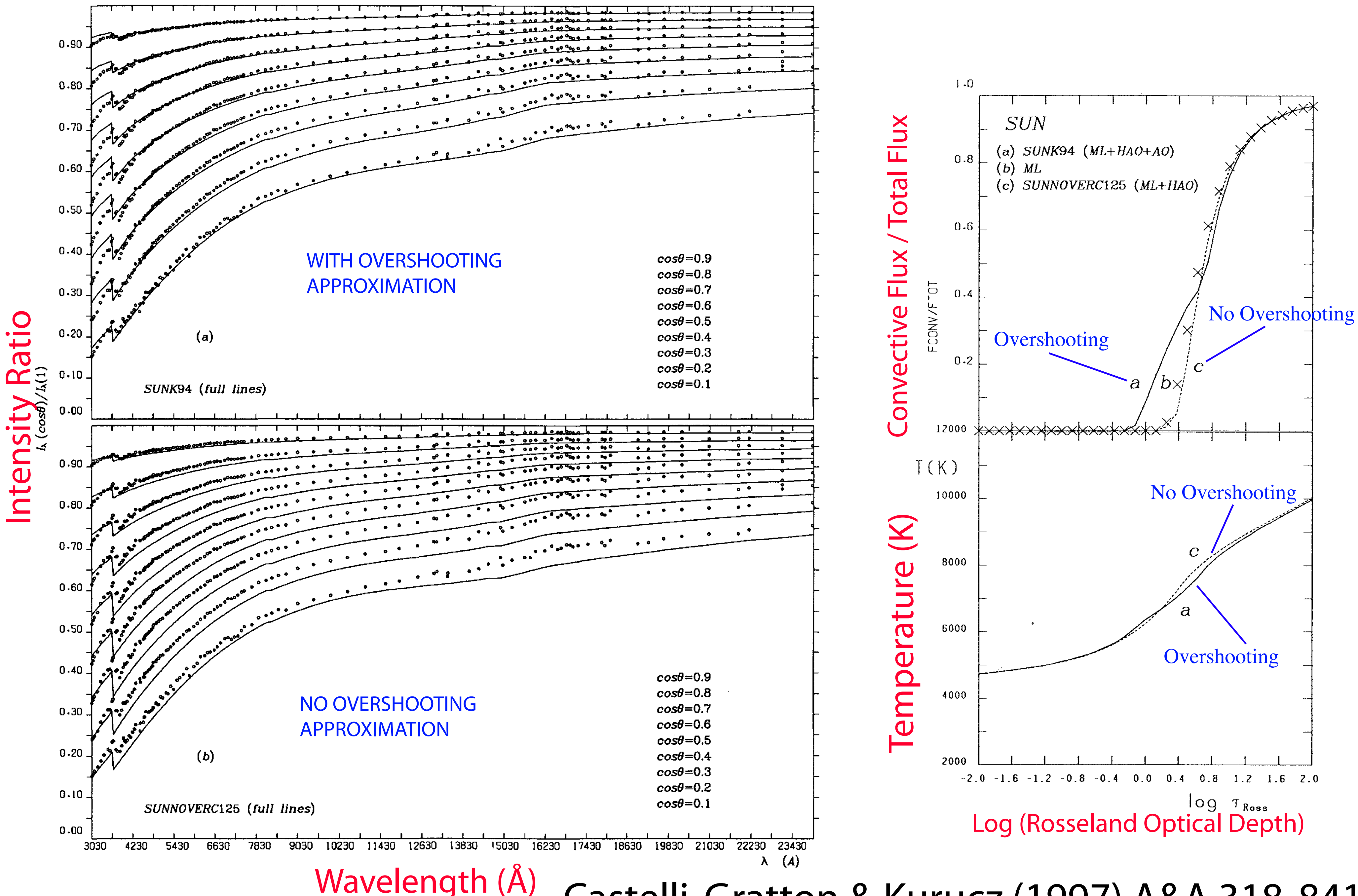

Castelli, Gratton & Kurucz (1997) A&A 318, 841

Temperature Structure Constrained by Interferometric Diameters

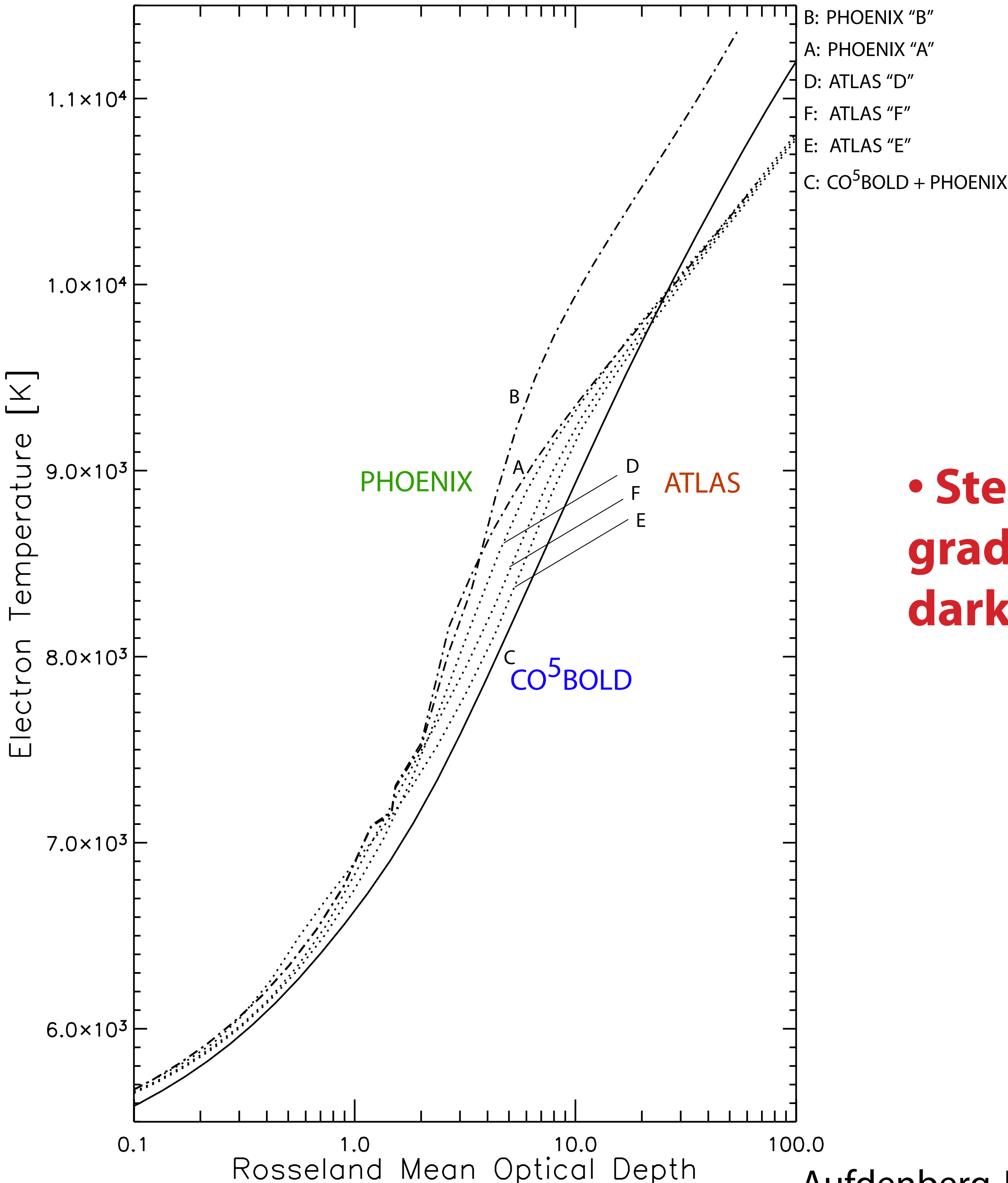

- **Steepness of temperature gradient determines limb darkening**

Aufdenberg, Ludwig & Kervella (2005) ApJ, 633, 424

Stars up close, More Than One Temperature Structure

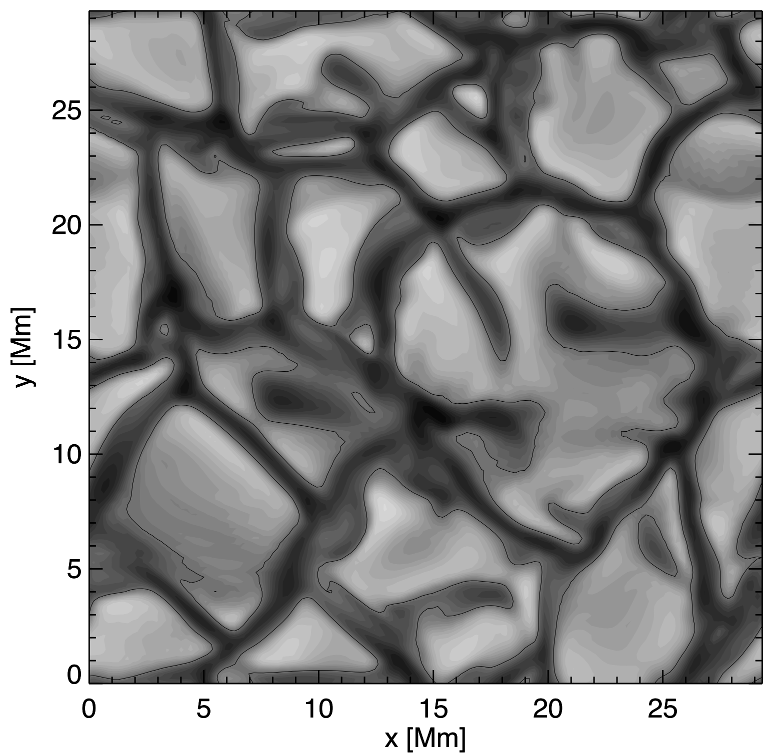

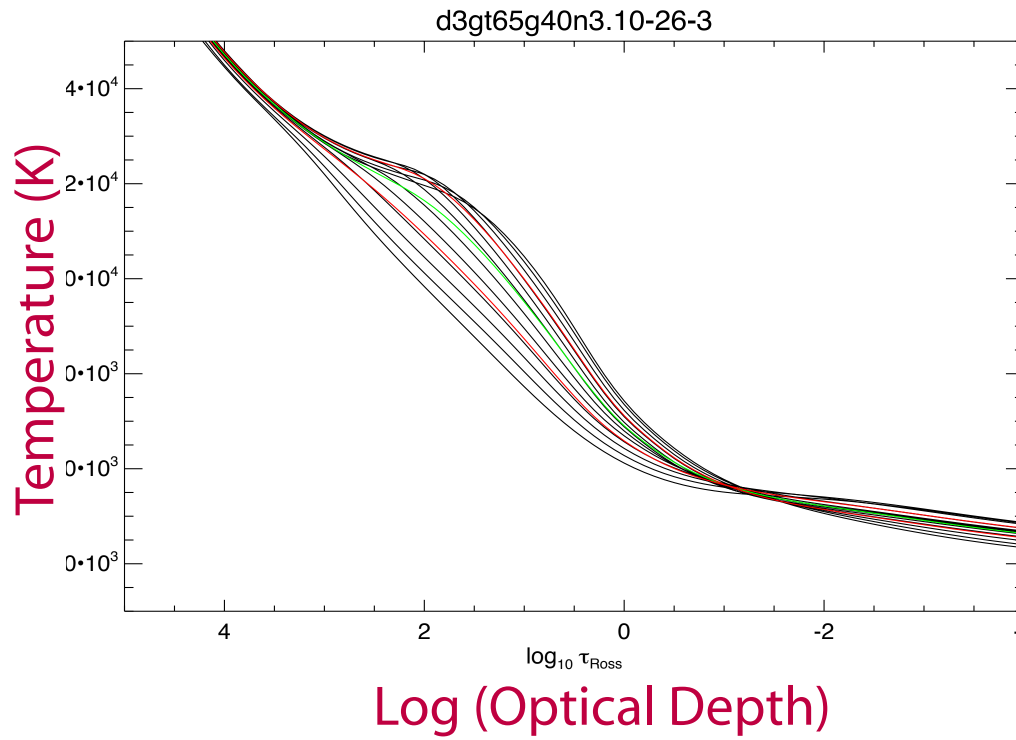

Hotter, rising granules have a warmer temperature structure than cooler, descending dark lanes.

Procyon: Aufdenberg, Ludwig & Kervella (2005) ApJ, 633, 424

Spectral Energy Distribution from 3-D Stellar Surfaces

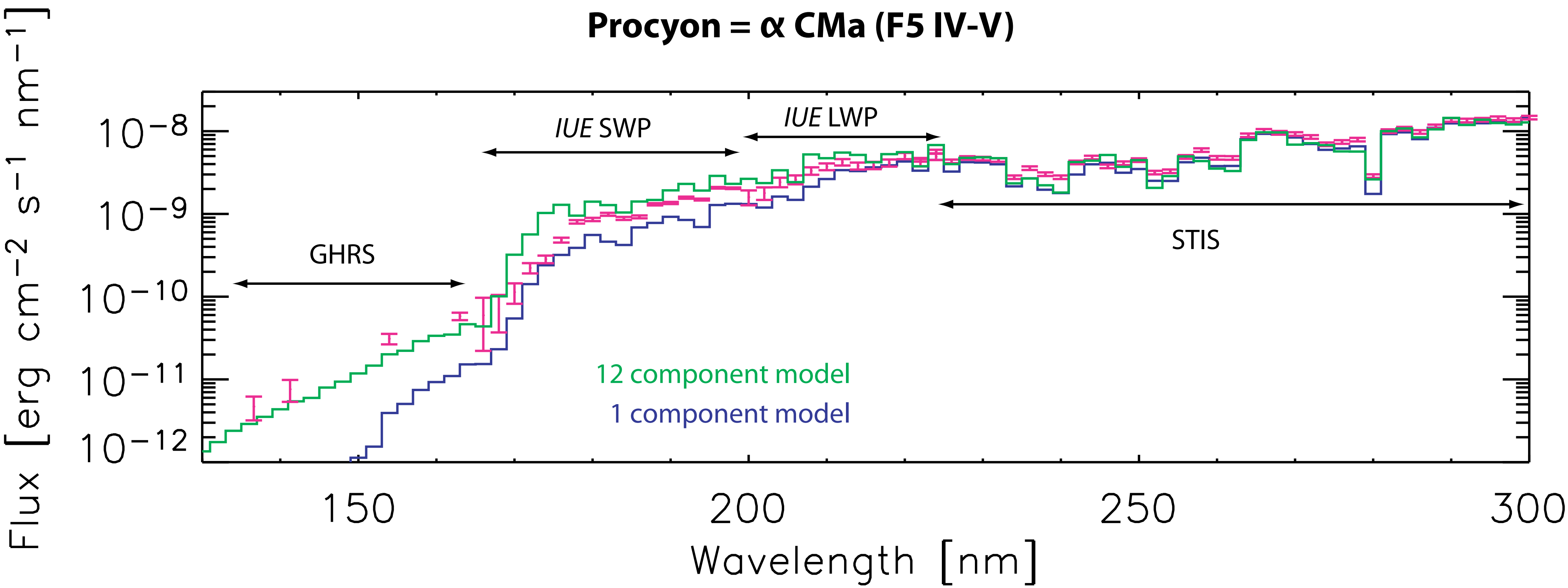

- **Multi-temperature component photosphere matches SED in the short ultraviolet, 1D model with overshooting does not**

Aufdenberg, Ludwig & Kervella (2005) ApJ, 633, 424

Solar spectral line strengths as a function of limb angle

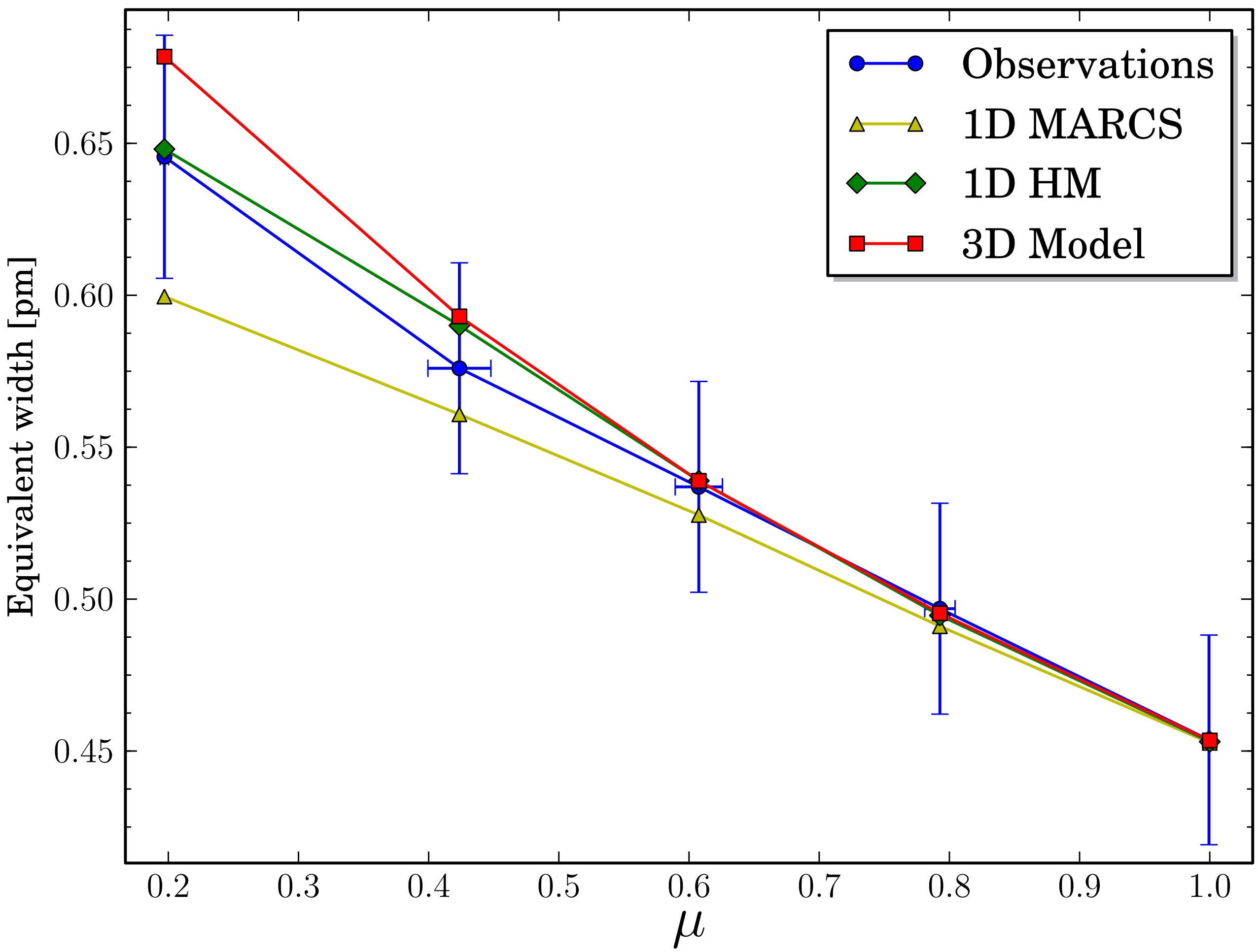

Fig. 9. Equivalent width vs. μ for the [O I]+Ni I 630.03 nm lines blend, for our observations and different models at different positions in the solar disk.

Pereira, Asplund & Kiselman (2009) A&A, 508, 1403

Diameter and photospheric structures of Canopus from AMBER/VLTI interferometry★,★★

A. Domiciano de Souza[1], P. Bendjoya[1], F. Vakili[1], F. Millour[2], and R. G. Petrov[1]

Canopus = α Car (F0Ib): H- and K -bands

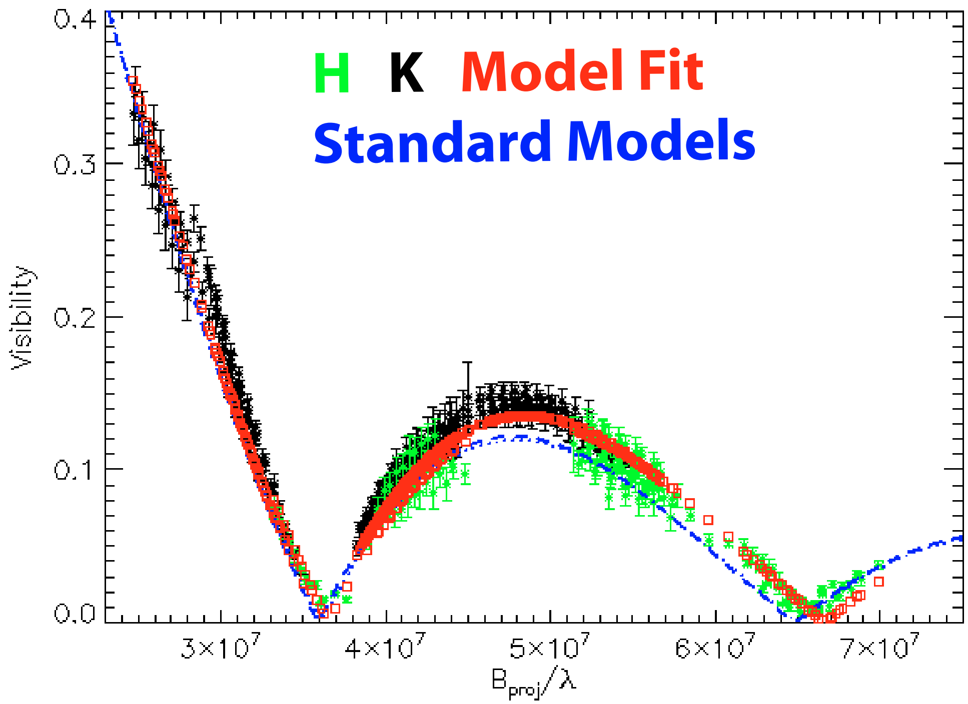

Non-Zero Closure Phase

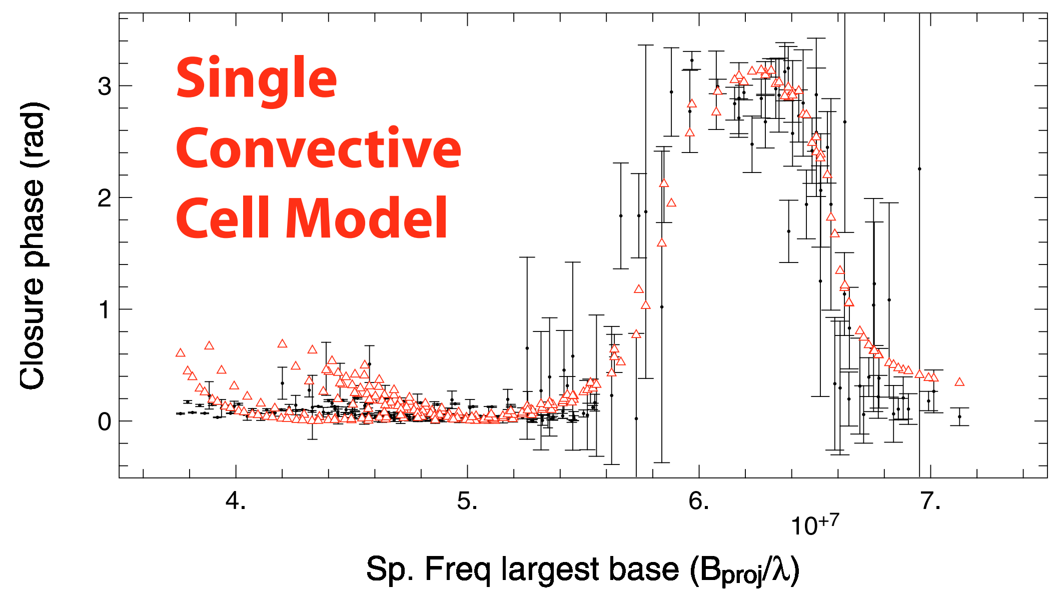

- **Canopus less limb darkened that expected from standard models**
- **Evidence for presence for convective cell**

Domiciano de Souza et al. (2008) A&A, 489, L8

EXTENDED ENVELOPES AROUND GALACTIC CEPHEIDS. III. Y OPHIUCHI AND α PERSEI FROM NEAR-INFRARED INTERFEROMETRY WITH CHARA/FLUOR

α Per (F5Ib): K-band UV coverage

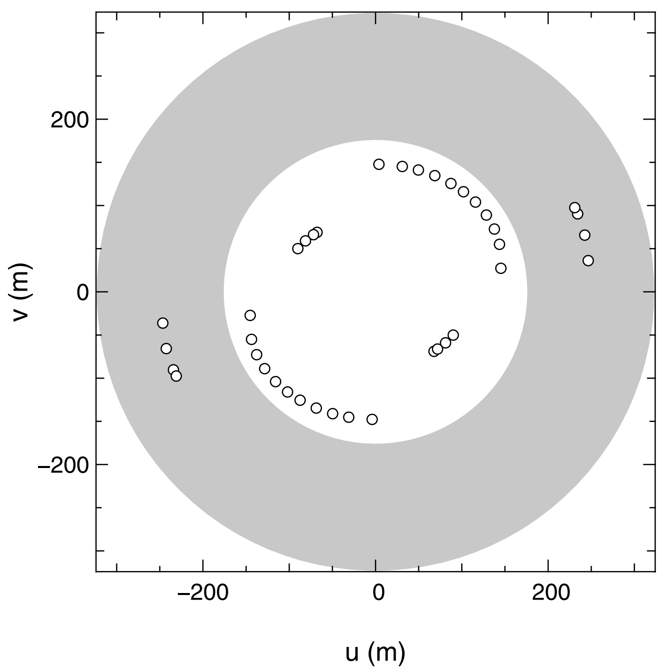

α Per (F5Ib): K-band Residuals to hydrostatic Model

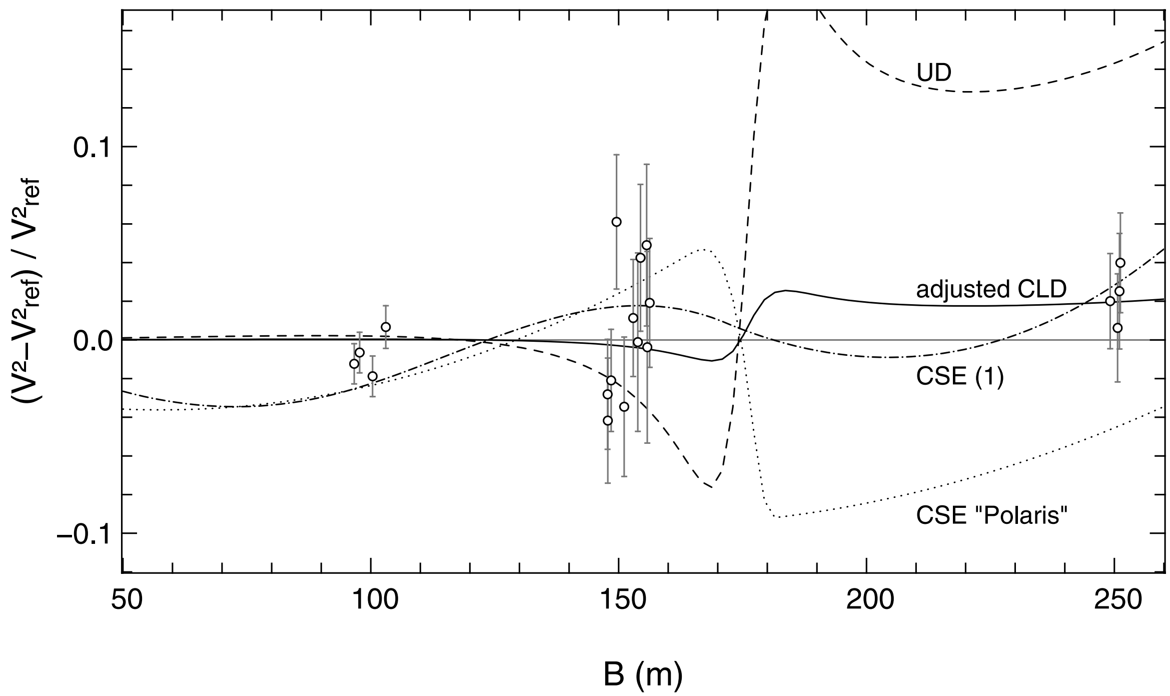

- **α Per also less limb darkened than spherical hyrdostatic models**

Mérand et al. (2007) ApJ, 664, 1093 [More about Cephieds @ 10:50!]

Radiative hydrodynamics simulations of red supergiant stars: II. simulations of convection on Betelgeuse match interferometric observations

A. Chiavassa[1,2], X. Haubois[3], J. S. Young[4], B. Plez[2], E. Josselin[2], G. Perrin[3], and B. Freytag[5,6]

IOTA data image reconstruction

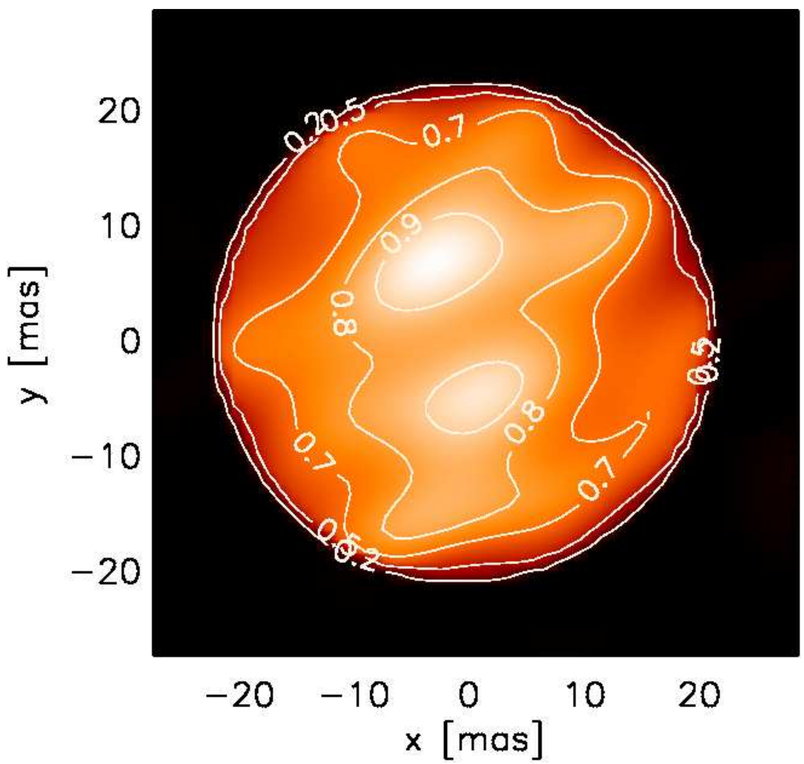

3D Simulation/Best match to V² and Closure phase data

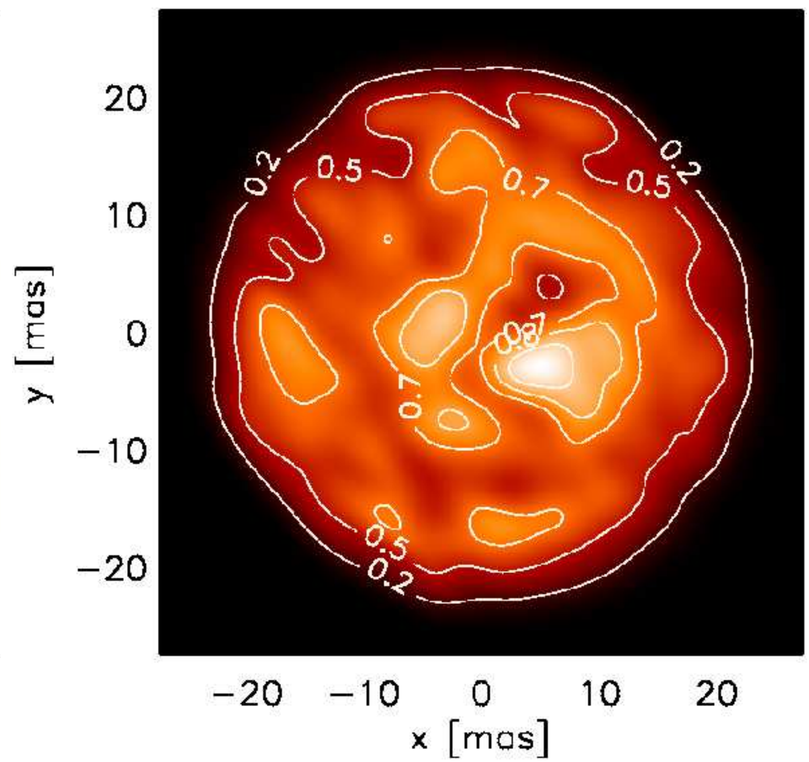

Chiavassa et al. (2010) A&A 515, 12 [more 3D Models @ 11:10!]

The spinning-top Be star Achernar from VLTI-VINCI

A. Domiciano de Souza[1], P. Kervella[2], S. Jankov[3], L. Abe[1], F. Vakili[1,3], E. di Folco[4], and F. Paresce[4]

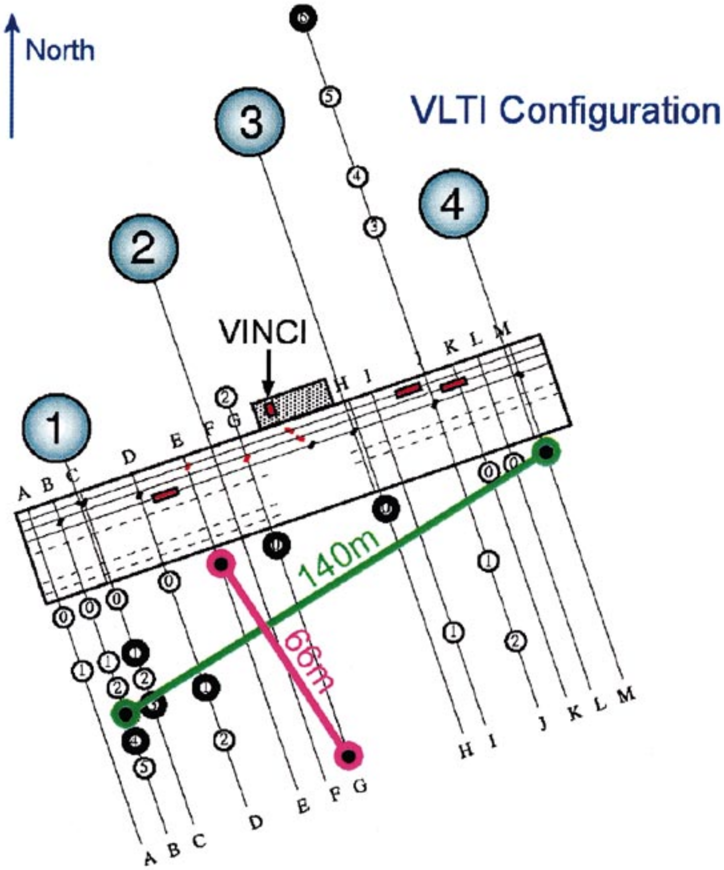

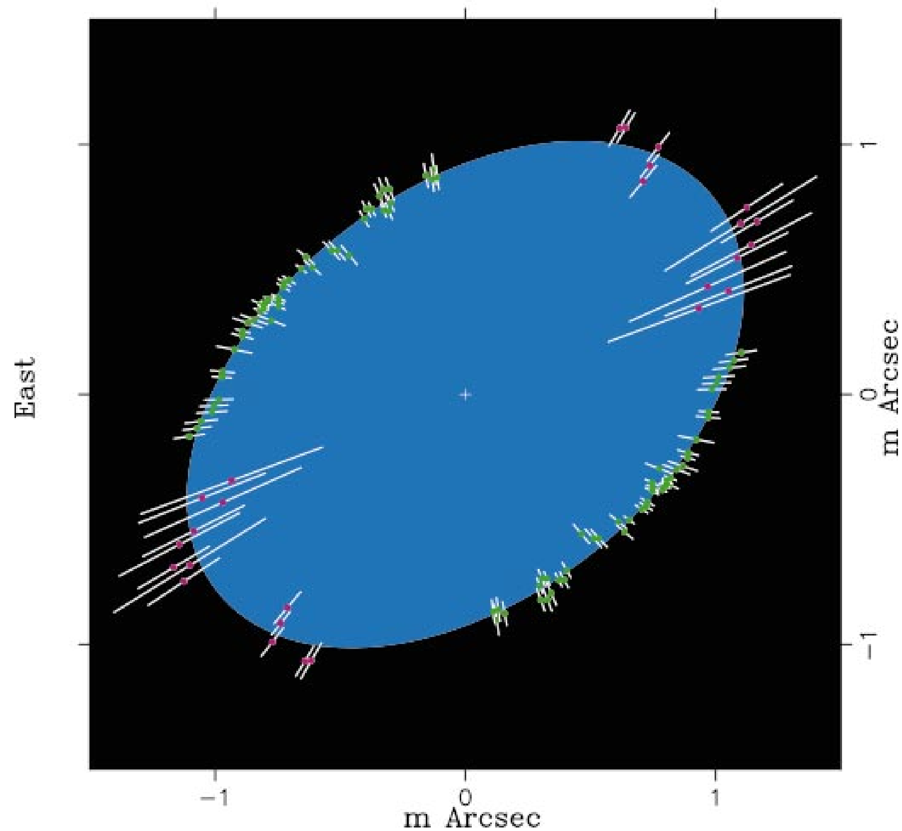

*Disk of **Achernar** (B3 Vpe) resolved as ellipsoid by VLTI (Axial ratio: 1.56±0.05

Domiciano de Souza et al. (2003) A&A, 407, L47 [More rotating stars @ 14:00!]

Theory of Rotating Stars Revitalized by Observations

Models for Achernar with Differential Rotation

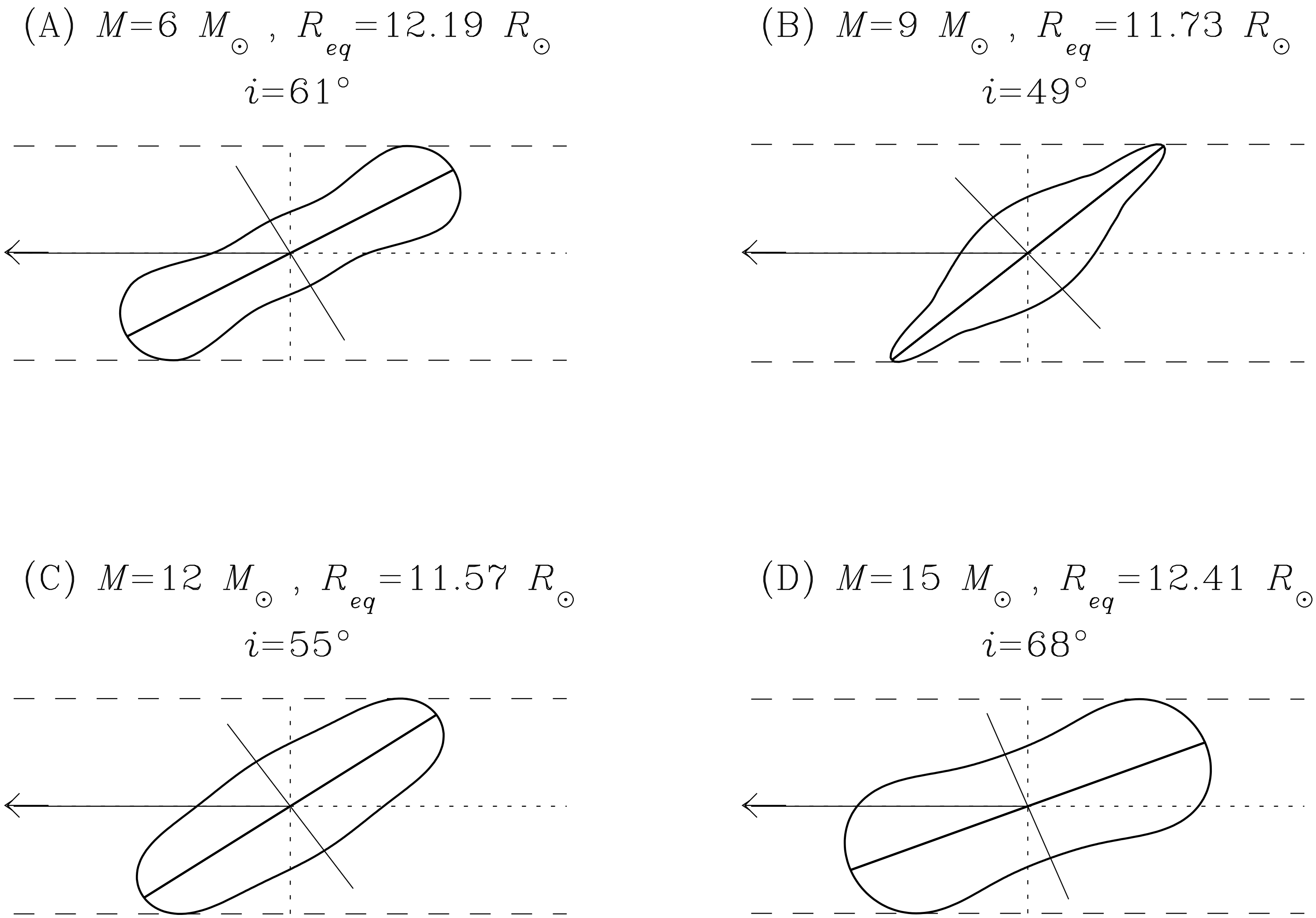

Jackson, MacGregor, Skumanich (2004) ApJ, 606, 1196

The polar wind of the fast rotating Be star Achernar

VINCI/VLTI interferometric observations of an elongated polar envelope

P. Kervella[1] and A. Domiciano de Souza[2,3]

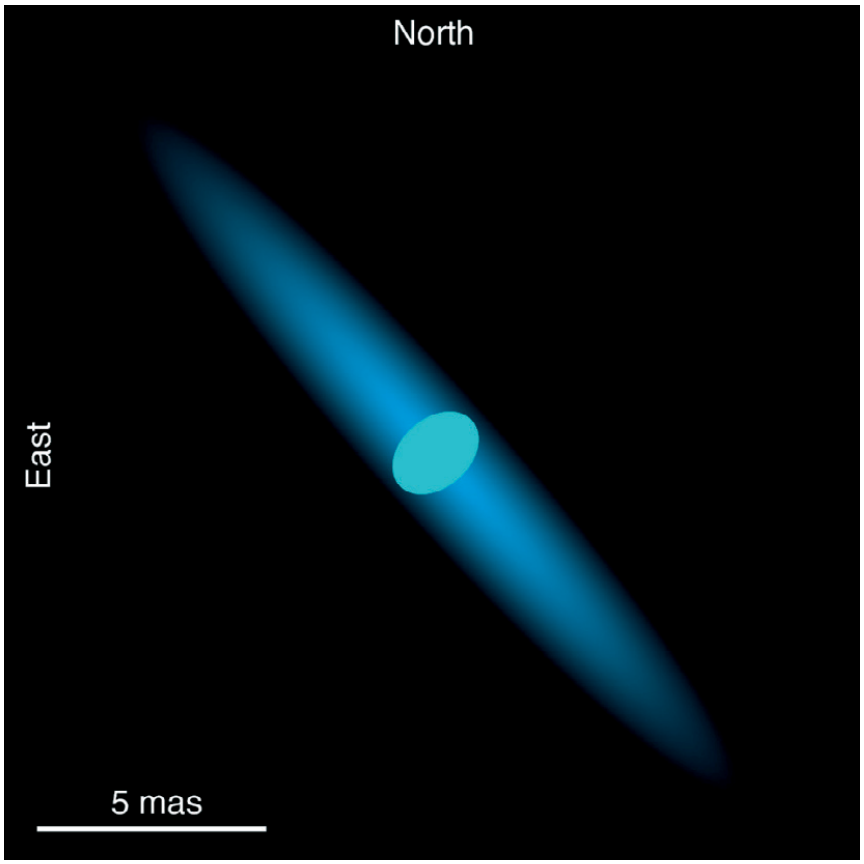

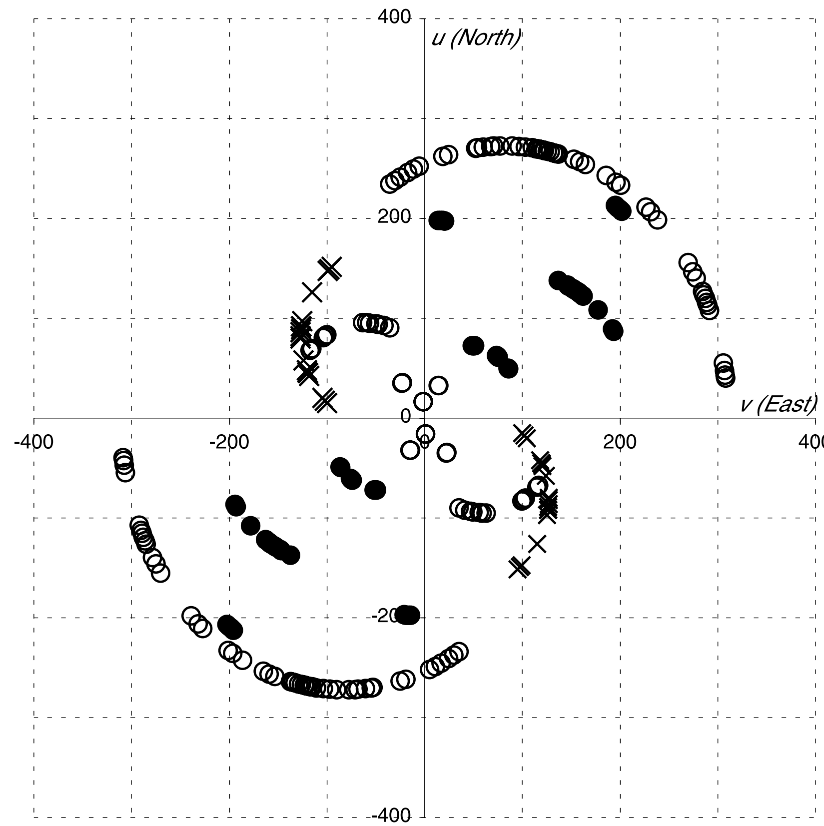

Kervella & Domiciano de Souza (2006) A&A, 453, 1059

The environment of the fast rotating star Achernar⋆

II. Thermal infrared interferometry with VLTI/MIDI

P. Kervella[1], A. Domiciano de Souza[2], S. Kanaan[2], A. Meilland[3], A. Spang[2], and Ph. Stee[2]

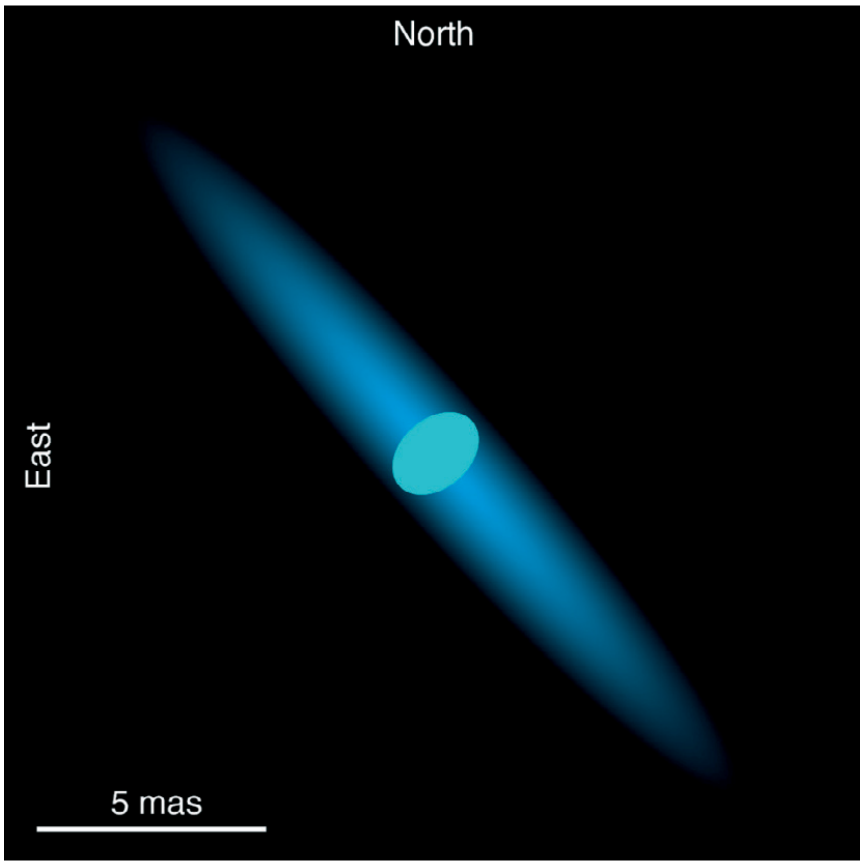

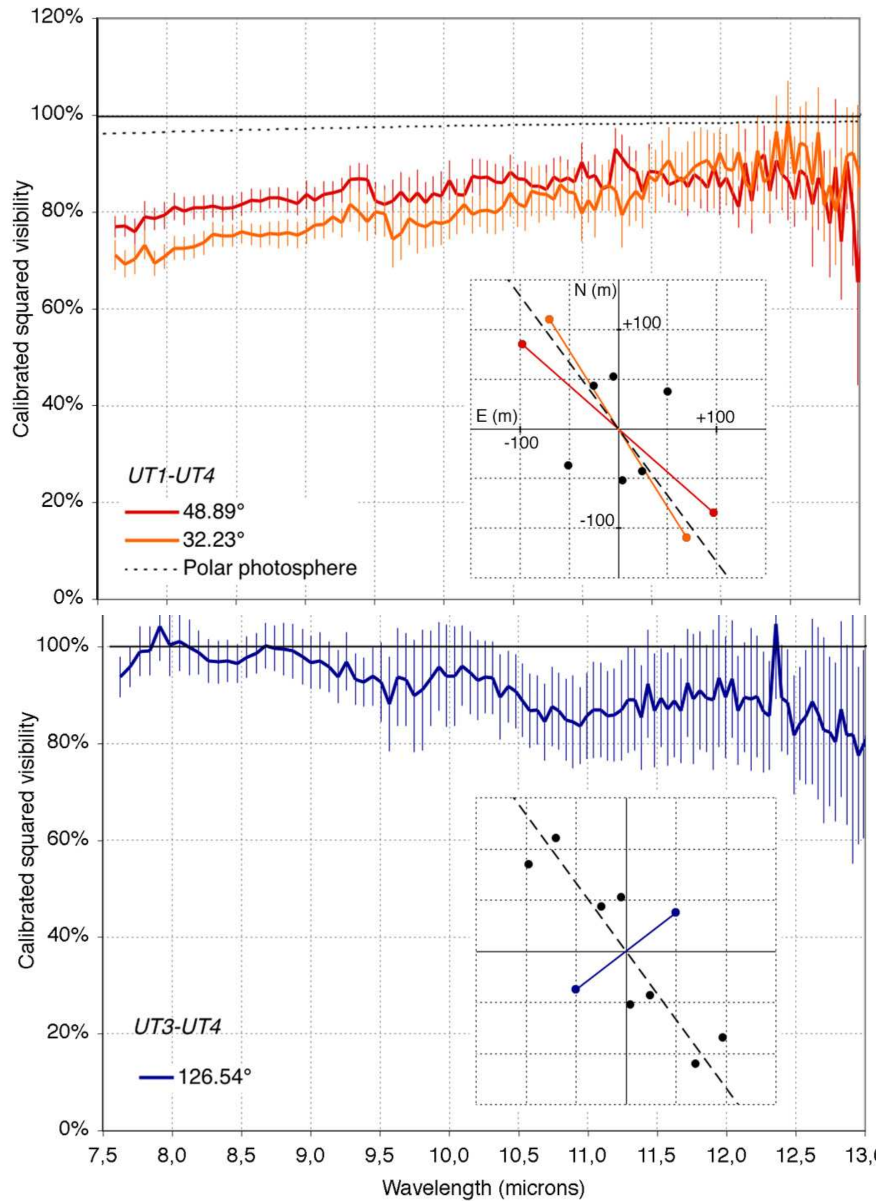

Kervella et al. (2009) A&A, 493, 53

Additional Resolved Rapid Rotating Stars from Interferometry

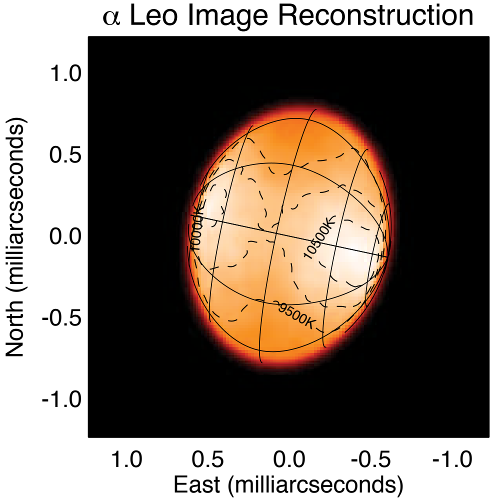

*Disk of **Regulus** (B7 V) resolved as ellipsoid by CHARA (McAlister et al. 2005, Che et al. 2011).

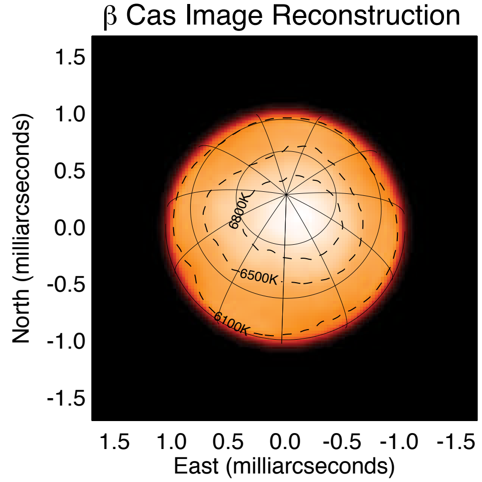

*Disk of **Caph** (F2 IV) resolved as ellipsoid by CHARA/MIRC (Che et al. 2011).

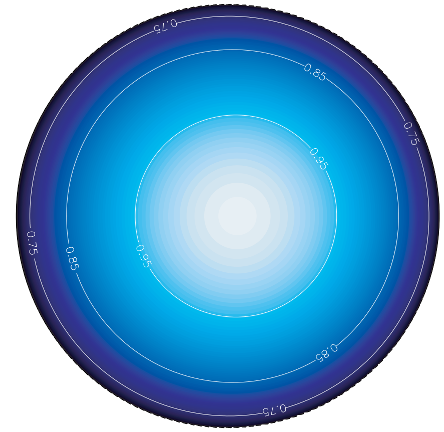

*Pole of **Vega** (A0 V) resolved by CHARA (Aufdenberg et al. 2006).

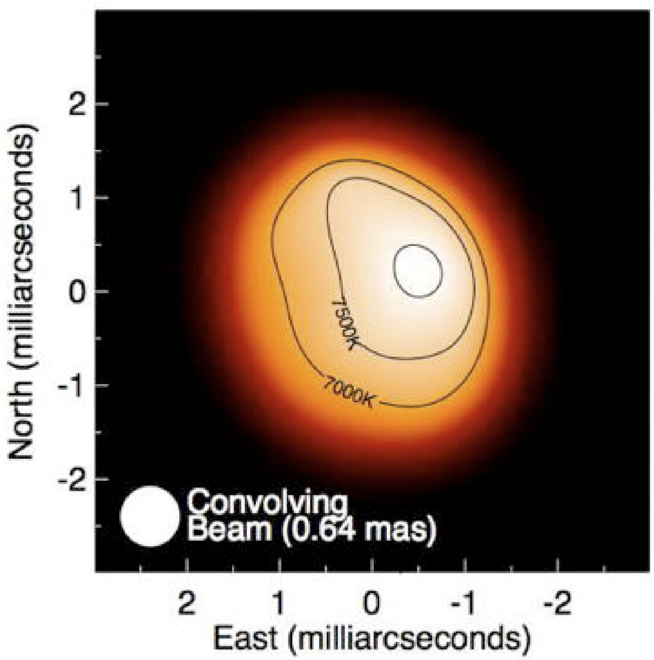

*Disk of **Altair** (A7 V) resolved by CHARA (J. Monnier et al. 2007).

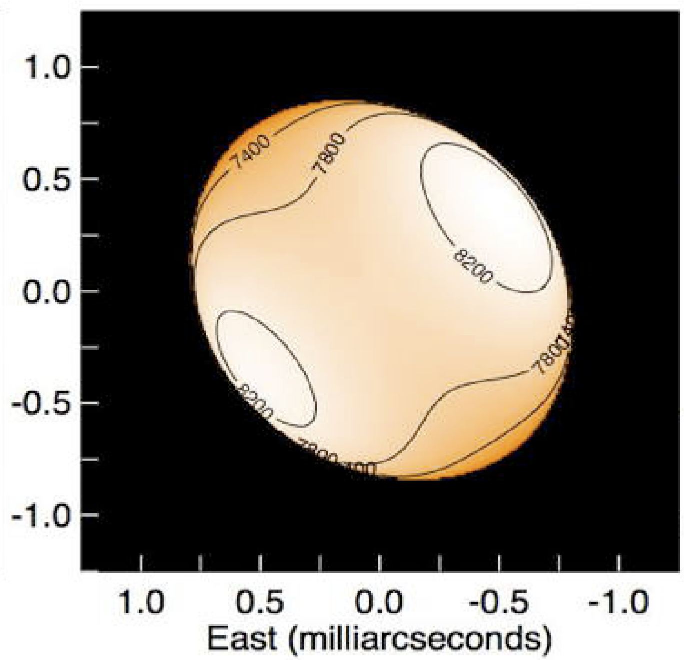

*Disk of **Alderamin** (A7 V) resolved by CHARA (M. Zhao et al. 2009).

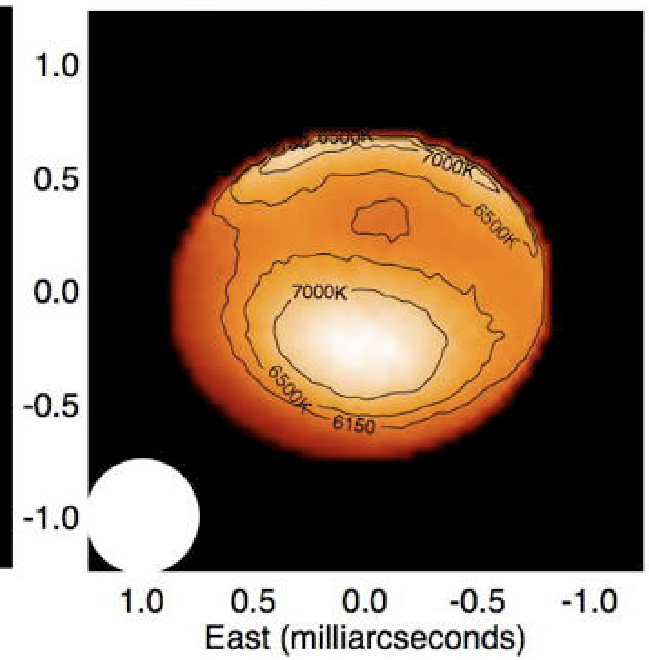

*Disk of **Rasalhague** (A5 III) resolved by CHARA (M. Zhao et al. 2009).

Gravity darkening in rotating stars

F. Espinosa Lara[1,2] and M. Rieutord[1,2]

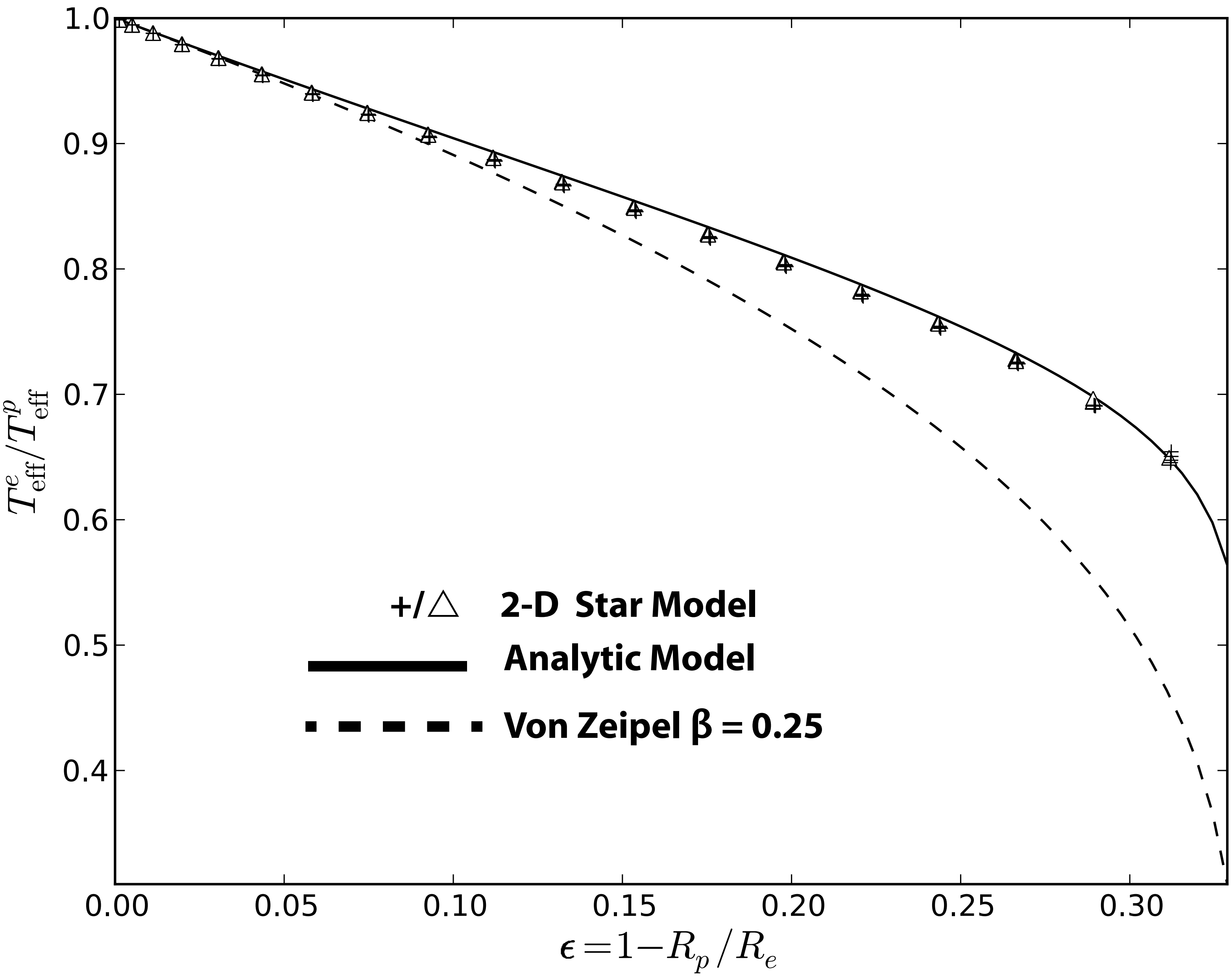

- **Observations by CHARA/ MIRC show gravity darkening weaker than β=0.25**

Espinosa Lara & Rieutord (2011) A&A, 533, 43

Limb and Gravity Darkening for Rotating Stars

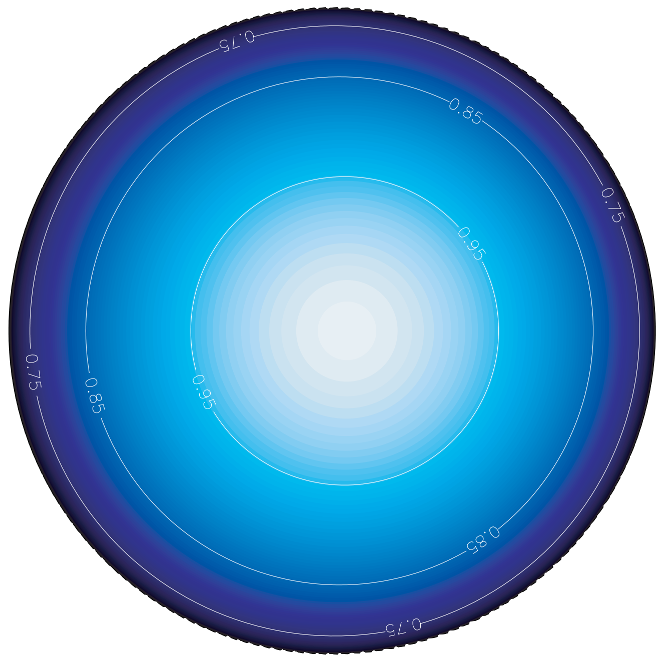

Pole-on view

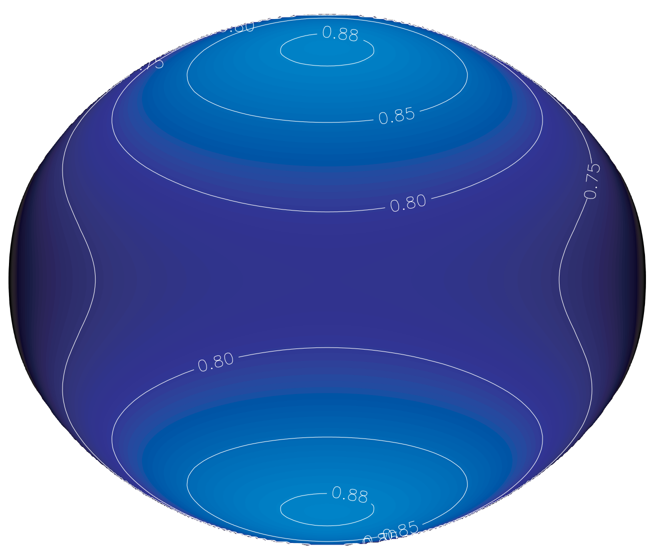

Equator-on view

Aufdenberg et al. (2006) ApJ, 645, 664

Self-Consistant Field (SCF) Model Limb and Gravity Darkening Movie

Aufdenberg & MacGregor, in preparation

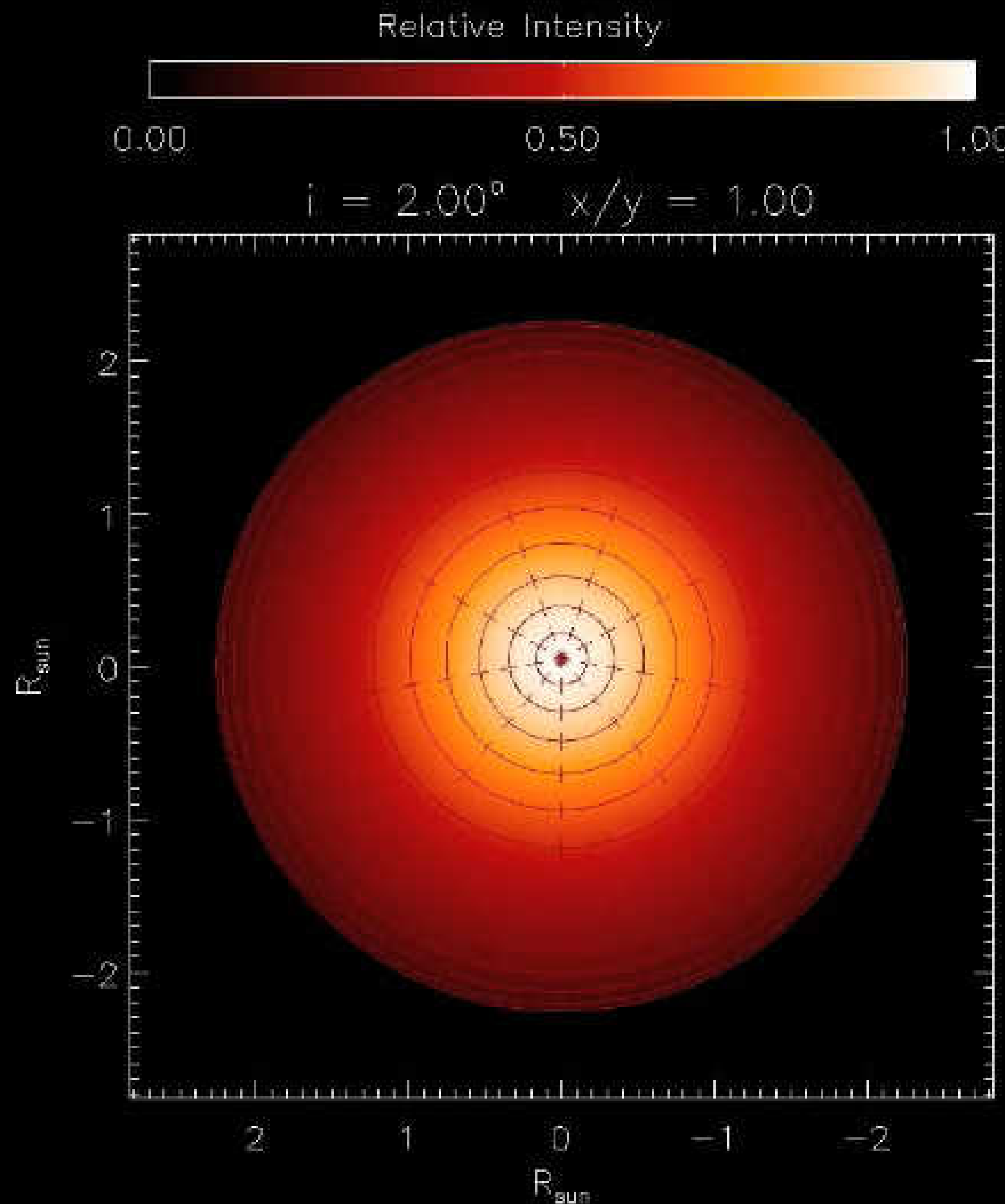

SCF Models: SEDs and Line Spectra Movie

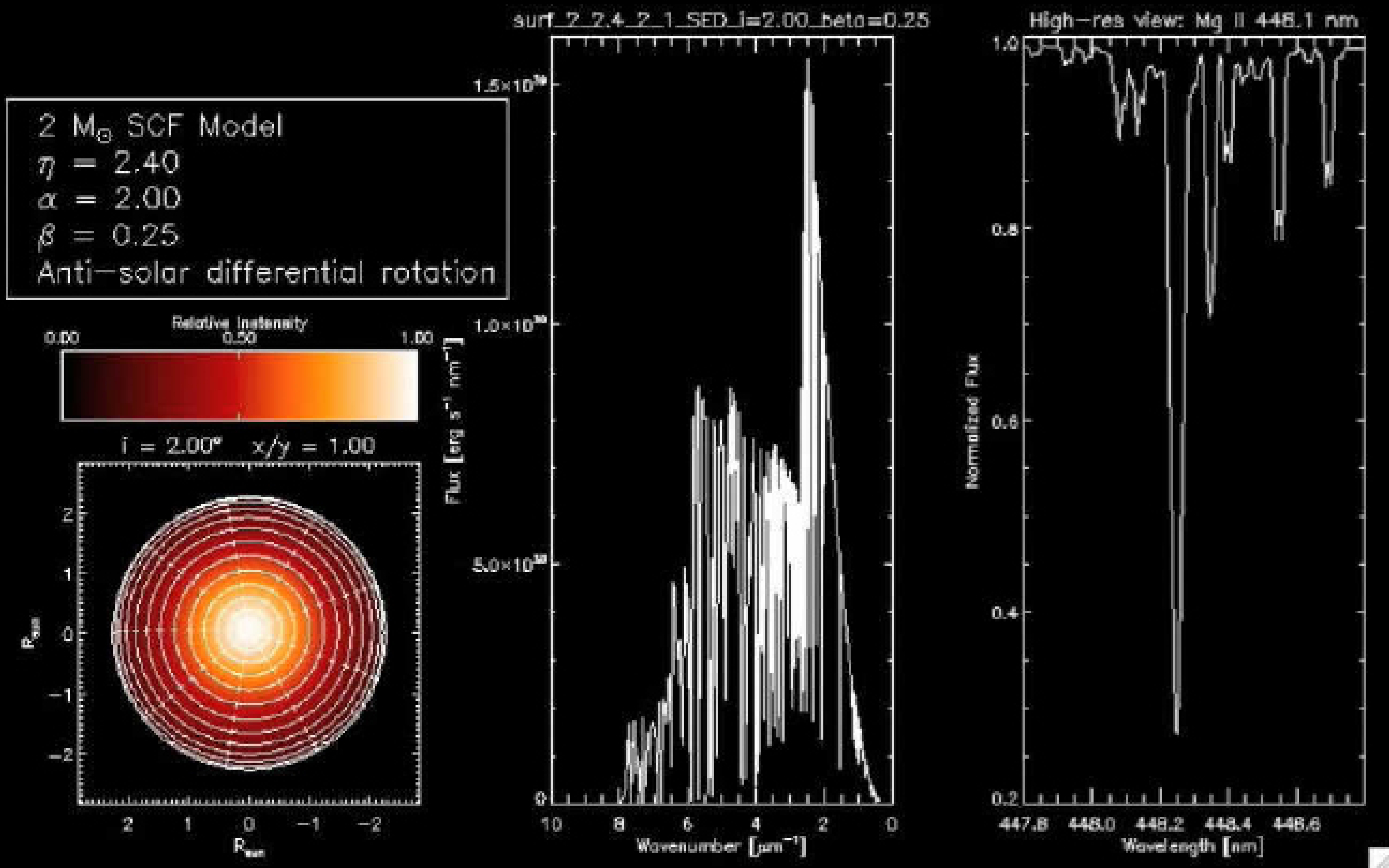

Aufdenberg & MacGregor, in preparation

Interferometry at visible wavelengths:

higher angular resolution --> O & B diameters & darkening

limb darkening more sensitive to temperature gradients

Thank you for your attention!